

---

Introduction to Paraunitary Filter Banks  
and Orthogonal Expansions in  $\ell^2$

---

by Prof. Dr. Dr. Daniel J. Strauss

# Contents

<b>1</b>	<b>Filter Banks and Adapted Time–Scale Atoms</b>	<b>3</b>
1.1	Introduction . . . . .	3
1.2	Multirate Signal Processing . . . . .	5
1.2.1	Downsampling and Decimation . . . . .	6
1.2.2	Upsampling and Interpolation . . . . .	8
1.2.3	The Polyphase Decomposition . . . . .	9
1.3	Two–Channel Filter Banks . . . . .	11
1.3.1	Critical Sampling and Perfect Reconstruction . . . . .	11
1.3.2	Polyphase Implementation . . . . .	14
1.3.3	Paraunitary Filter Banks . . . . .	16
1.4	Multiresolution Decompositions of $\ell^2$ . . . . .	18
1.4.1	Orthonormal Expansions via Filter Banks . . . . .	19
1.4.2	Octave–Band Decomposition . . . . .	20
1.4.3	Generalized Binary Tree Decompositions . . . . .	24
1.5	Signal–Adapted Filter Banks . . . . .	27
1.5.1	Lattice Structure Based Filter Banks . . . . .	28
1.5.2	Lattice Optimization by Genetic Algorithms . . . . .	33
1.6	Conclusions . . . . .	37
	<b>Bibliography</b>	<b>39</b>



# Chapter 1

## Filter Banks and Adapted Time–Scale Atoms

*The theory of signal–adapted filter banks has been developed in signal compression in recent years. Up to now, the underlying ideas mainly stick on this restricted area although they may have merit in other application fields such as machine learning. In this chapter, we introduce lattice structure based signal–adapted filter banks and time–scale atoms, respectively, which we extensively employ in the subsequent chapters for their new application in machine learning instead of signal compression. For decompositions by time–scale atoms, we strictly make use of a discrete–time approach which is well suited for digital signal processing. For the sake of self–consistency, we review the theory of paraunitary filter banks, describing how they are related to multiresolution decomposition of  $\ell^2$ .*

### 1.1 Introduction

Digital signal processing plays undoubtedly a major role in modern technology such as in communications, acoustic, speech, and image processing or the biomedical area. A particular interesting branch of digital signal processing is called multirate signal processing. Over the last two decades, there has been a tremendous growth of research in this area and the design of multirate systems. The basic signal transformation in multirate signal processing is by means of filter banks. Here a signal is decomposed into different frequency bands along with appropriate manipulations of the sampling rate.

Such spectral decompositions are the essence of the so-called *subband coding* [9, 76] and are closely related to signal decompositions by time<sup>1</sup>–scale atoms, in particular, wavelets which have originally been introduced in the mid 1980s for the analysis of seismic data [21] to provide a time–scale (or time–frequency) representation of signals. In contrast to the windowed Fourier transform, wavelet analysis allows for an analysis with a variable window in the time–scale domain such that often a good compromise between the time and frequency resolution, determined by Heisenberg’s uncertainty principle, can be achieved. As we will see, filter banks are in many cases directly related to wavelet decompositions.

A question that naturally arises in this context is the choice of wavelets and filter banks, respectively, that are ideally suited for a given task. The design of wavelets and filter banks which are optimal for signal compression has been addressed by several authors, e.g., see [12, 67] for some initial approaches, and a strong theoretical framework for signal–adapted filter banks has been developed in recent years [42, 72]. Up to now, the underlying ideas mainly stick on this restricted area.

In recent studies, we have shown that an adaptation technique from signal compression is an effective tool for real world pattern recognition tasks when using appropriate class separability criteria instead of coding conditions [28, 29, 28, 26, 27, 30, 31, 32, 26, 62, 60, 61, 63, 65, 64]. In this chapter, we present the necessary foundation for signal–adapted filter banks based on lattice structures which have not been used in pattern recognition up to now. We present a detailed review on paraunitary filter banks, describing how they are related to orthonormal decompositions of  $\ell^2$ .

A filter bank adaptation based on lattice structure rises up an optimization problem in the space of lattice angles. We introduce two techniques to tackle with this problem, namely the  $\mu$ –*orthogonality* and *genetic algorithms*. These methods are ideally suited for settings where sophisticated calculus based optimization strategies cannot be applied. Such settings typically appear for our waveform recognition tasks in the subsequent chapters.

**Organization.** In Section 1.2 we present the necessary fundamentals of multirate signal processing. Section 1.3 introduces two–channel filter banks, with a special focus on paraunitary filter banks. In Section 1.4 we describe wavelet–like decompositions

---

<sup>1</sup>It goes without saying that the term ‘time’ can be used interchangeably with ‘space’ when dealing with spatial rather than time dependent signals.

of  $\ell^2$  by time-scale atoms. Section 1.5 introduces the lattice structure in detail. We also present two optimization (or adaptation) strategies for time-scale atoms in this section. The conclusions of the chapter are given in Section 1.6.

## 1.2 Multirate Signal Processing

Discrete-time signals are usually considered as vectors  $\mathbf{x} \in \mathbb{R}^d$  or sequences  $\mathbf{x} \in \ell^2$  with samples  $x[\cdot]$ . Unless stated otherwise, we assume the latter throughout this chapter. In general, a discrete-time signal is obtained by the periodic sampling of a continuous-time signal  $s(t)$  ( $t \in \mathbb{R}$ ) with sampling period  $T_s$  such that

$$x[\cdot] = s(\cdot T_s), \quad T_s \in \mathbb{R}.$$

The sampling period gives the sampling frequency  $\Omega_s = 2\pi/T_s$ . Clearly,  $\mathbf{x}$  can only be an exact representation of  $s(\cdot)$  if the sampling theorem is fulfilled. In the following, we will show how we can change the sampling rate of  $\mathbf{x}$  to obtain a new signal  $\mathbf{y}$ . Such manipulations of the sampling rate are often desirable in discrete-time systems. It goes without saying that this can always be seen as a new representation of the underlying continuous signal with  $y[\cdot] = s(\cdot \bar{T}_s)$  where  $\bar{T}_s \neq T_s$ . Let us denote the frequency variable of continuous-time signals by  $\Omega$  [rad/s] and of discrete-time signals by  $\omega$  [rad]. We use capital letters when the signals are represented in Fourier domain and  $z$ -domain. In other words, for a sequence  $\mathbf{x}$  we have that  $X(e^{i\omega}) = \sum_{n \in \mathbb{Z}} x[n]e^{-i\omega n}$  and  $X(z) = \sum_{n \in \mathbb{Z}} x[n]z^{-n}$ , respectively. We will also use the discrete-time Fourier series for  $M$ -periodic sequences with the analysis equation  $X[k] = \sum_{n=0}^{M-1} x[n]W_M^{kn}$  where  $W_M = e^{-i2\pi/M}$  denotes the  $M$ th root of unity and the synthesis equation  $x[n] = M^{-1} \sum_{k=0}^{M-1} X[k]W_M^{-kn}$ .

Note that we have the normalization  $\omega = T_s \Omega$  if  $\mathbf{x}$  was obtained by sampling  $s(\cdot)$  with  $T_s$ . Throughout this thesis we, will restrict our interest almost exclusively on the discrete-time signal and assume without a word that the underlying continuous signal is sampled properly. There exists rich literature on multirate signal processing, e.g., see [3, 70, 17, 76, 59], where the theory can be found. However, there is a broad lack of standardization in this literature concerning terms, sign conventions, system theoretical conventions such as the consideration of causality and so on. Here we pick out only those elements from the theory which are needed for the subsequent chapters

using uniform notations and conventions which are most appropriate for our purpose and to receive consistency. Therefore, our notation differs in other books on the topic. The notation of system theoretical facts follows the standard work on discrete-time signal processing by Oppenheim and Schaffer [44].

### 1.2.1 Downsampling and Decimation

*Downsampling* by an integer factor of  $M$  denotes a reduction of the sampling rate of  $\mathbf{x}$  such that a new sequence  $\mathbf{y}$  is obtained by

$$y[\cdot] = x[M\cdot]. \quad (1.2.1)$$

Let  $x'[n]$  be  $x[n]$  for  $n = 0, \pm M, \pm 2M, \dots$  and zero otherwise and let  $\delta[\cdot]$  be *unit impulse*, i.e., we have that  $\delta[n] = 1$  if  $n = 0$  and  $\delta[n] = 0$  else. By introducing the impulse sequence  $v[\cdot] = \sum_{l \in \mathbb{Z}} \delta[\cdot - lM]$  we have that  $x'[\cdot] = x[\cdot]v[\cdot]$ . Note that the discrete-time Fourier series expansion coefficients of  $\mathbf{v}$  are given by  $V[k] = \sum_{n=0}^{M-1} \delta[n]W_M^{nk} = 1$  ( $k \in \mathbb{Z}$ ) such that the Fourier series of  $\mathbf{v}$  reads  $v[n] = M^{-1} \sum_{k=0}^{M-1} W_M^{-kn}$  ( $n \in \mathbb{Z}$ ). Consequently, we have that  $x'[n] = M^{-1} \sum_{k=0}^{M-1} x[n]W_M^{-kn}$  ( $n \in \mathbb{Z}$ ) which yields

$$\begin{aligned} X'(z) &= \sum_{n \in \mathbb{Z}} x'[n]z^{-n} \\ &= \frac{1}{M} \sum_{k=0}^{M-1} \sum_{n \in \mathbb{Z}} x[n]W_M^{-kn} z^{-n} \\ &= \frac{1}{M} \sum_{k=0}^{M-1} X(zW_M^k). \end{aligned}$$

For  $\mathbf{y}$  we have that

$$Y(z) = \sum_{n \in \mathbb{Z}} x'[Mn]z^{-n} = X'(z^{\frac{1}{M}})$$

and finally, using our results above, the representation of  $\mathbf{y}$  in the  $z$ -domain is given by

$$Y(z) = \frac{1}{M} \sum_{k=0}^{M-1} X(z^{\frac{1}{M}} W_M^k). \quad (1.2.2)$$

Clearly, the process of discarding samples in (1.2.1) can lead to a loss of information. In the frequency domain this is reflected in the *aliasing effect*. To see this, consider

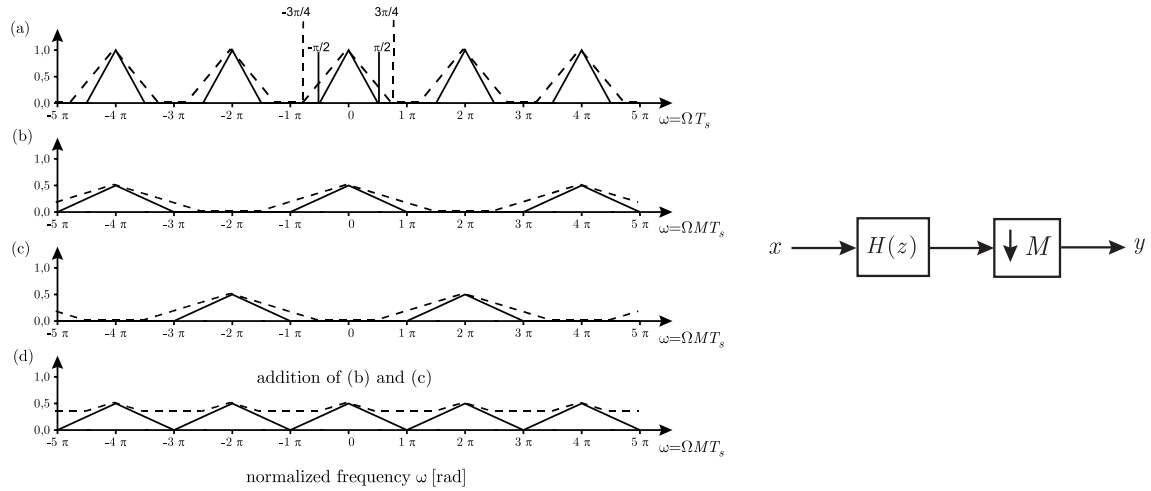


Figure 1.1: Left hand: Downsampling with and without aliasing for  $M = 2$  in the frequency domain. (a) Spectra of two baseband signals of different bandwidths. The signal shown as solid line satisfies  $|\omega| < \pi/M$  whereas the dashed signal does not. (b) The scaled versions  $\frac{1}{2}|X(e^{i\omega/2})|$  of the signals. (c) The shifted replica of the signals in (b), i.e.,  $\frac{1}{2}|X(e^{i(\omega-2\pi)/2})|$ . (d) The addition of the signals in (b) and (c) which results in aliasing for the dashed signal. Right hand: the  $M$ -fold decimator.

(1.2.2) on the unit circle and note that the Fourier transform  $X(e^{i\omega})$  of  $\mathbf{x}$  is scaled by a factor of  $M$  in frequency to obtain  $M^{-1}X(e^{i\omega/M})$  of periodicity  $2\pi M$ .  $Y(e^{i\omega})$  is given by the sum of  $M^{-1}X(e^{i\omega/M})$  and its  $M - 1$  frequency shifted versions  $M^{-1}X(e^{i(\omega-2\pi k)/M})$ , ( $k = 2, \dots, M$ ), the so-called *alias components*. Note that these alias components are shifted by  $2\pi$  to each other. For baseband signals this means that if  $M^{-1}X(e^{i\omega})$  is not bandlimited to  $|\omega| < \pi/M$ , i.e.,  $|X(e^{i\omega})| = 0 \forall |\omega| \geq \pi/M$  is not satisfied, this summation results in aliasing since the spectra do overlap. Figure (1.1) (left hand) shows the situation graphically for  $M = 2$ .

Thus it is straightforward to apply a filter which ensures that a signal is sufficiently bandlimited. Filtering followed by downsampling is called *decimation*. The whole process is symbolized by the scheme Figure 1.1 (right hand). We call this scheme a *M-fold decimator* if downsampling by factor  $M$  is applied. The symbol with the down-arrow is called a *M-fold downsampler* which implements the downsampling operation.  $H(z)$  is a LTI filter, also called *convolution filter* in mathematics, which is characterized by its impulse response  $\mathbf{h}$  or its transfer function  $H(z) = \sum_{n \in \mathbb{Z}} h[n]z^{-n}$ , respectively. We call this filter a *decimation filter*. Let  $*$  denote the *convolution product* such that

$y[\cdot] = (x * h)[\cdot] = \sum_{n \in \mathbb{Z}} x[n]h[\cdot - n]$ . Then the relation between  $\mathbf{y}$  and  $\mathbf{x}$  of a  $M$ -fold decimator is given by

$$y[\cdot] = (x * h)[M\cdot]. \quad (1.2.3)$$

### 1.2.2 Upsampling and Interpolation

*Upsampling* by an integer factor of  $L$  denotes an increase of the sampling rate of  $\mathbf{x}$  such that a new sequence  $\mathbf{y}$  is obtained by

$$y[\cdot] = \sum_{k \in \mathbb{Z}} x[k]\delta[\cdot - kL], \quad (1.2.4)$$

which directly yields the representation in the  $z$ -domain

$$Y(z) = \sum_{n \in \mathbb{Z}} \left( \sum_{k \in \mathbb{Z}} x[k]\delta[n - kL] \right) z^{-n} = X(z^L). \quad (1.2.5)$$

Vaidyanathan [69] has graphically interpreted (1.2.5) as follows: on the unit circle we have that  $Y(e^{i\omega}) = X(e^{i\omega L})$ . This can be seen as the graph of a basic spectrum of periodicity  $2\pi$  which is a  $L$ -fold compressed version of  $X(e^{i\omega})$ . But the the graph  $Y(e^{i\omega})$  also contains  $L - 1$  frequency shifted copies of this basic spectrum, the so-called *images*. The appearance of these images is called the *imaging effect*, see Figure 1.2 (left hand) for an illustration of imaging. As we will see later, removing these images from  $Y(e^{i\omega})$  by means of filtering is often desirable in discrete-time systems. Upsampling followed by filtering is called *interpolation*. The resulting scheme is shown in Figure 1.2 (right hand) and is called  *$L$ -fold interpolator* if upsampling by a factor  $L$  is applied.

Here  $G(z)$  is a LTI filter and is known as *interpolation* or *antiimaging filter*. The system with the up-arrow is called a  *$L$ -fold upsampler*. Finally, the process of  $L$ -fold interpolation in the time-domain reads

$$y[\cdot] = \left( \left( \sum_{k \in \mathbb{Z}} x[k]\delta[\cdot - kL] \right) * g \right) [\cdot] = \sum_{k \in \mathbb{Z}} x[k]g[\cdot - kL]. \quad (1.2.6)$$

Note that neither the downsampler nor the upsampler are time-invariant systems by (1.2.1) and (1.2.4), respectively. Due to (1.2.1) we have that  $y[n] = x[Mn]$  which for  $M > 1$ ,  $n > 0$  results in  $Mn > n$ . From (1.2.4) we have that  $y[n] = x[n/L]$  which for  $n = -L, -2L$  and  $L > 1$  implies  $n/L > n$ . This shows that these systems are also not causal (when leaving the consideration of a physical time scaling).

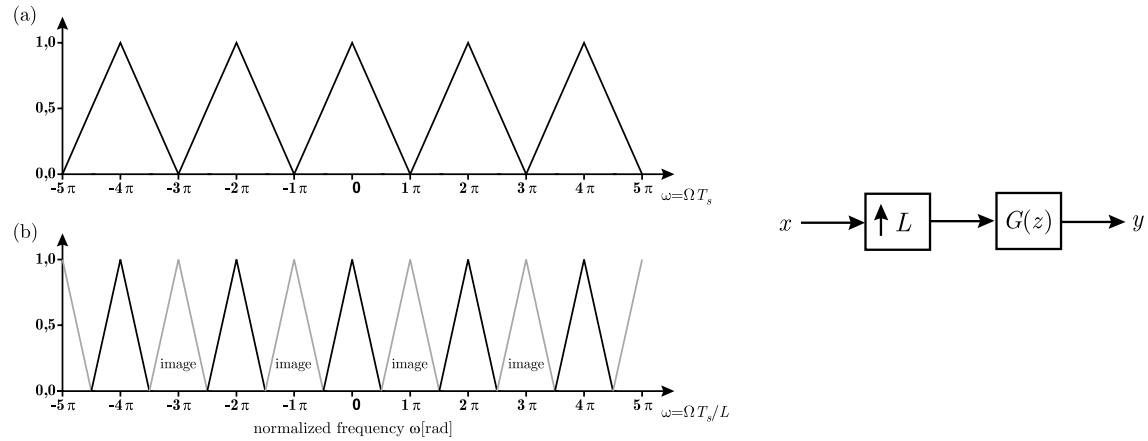


Figure 1.2: Left hand: the imaging effect for  $L = 2$ . (a) Spectrum of the original signal  $|X(e^{i\omega})|$ . (b) Spectrum  $|Y(e^{i\omega})|$  of the upsampled signal which shows the imaging effect. Right hand: the  $L$ -fold interpolator.

### 1.2.3 The Polyphase Decomposition

A cornerstone in the theory and practice of multirate signal processing is the invention of the polyphase decomposition [6, 74]. It simplifies the theory and allows for an efficient implementation of decimators and interpolators. Especially, for the efficient realization of multirate filter banks it is well suited as we will see.

**Noble Identities.** Before introducing the polyphase decomposition, let us have a look at the *noble identities* [69, 59] which will turn out to be very useful for our further discussions.

The first noble identity aims at decimation filters of a special form. Suppose we want to decimate a signal  $X(z)$  by a factor of  $M$  and a decimation filter  $\mathbf{h}$  that has  $M - 1$  zeros between its consecutive nonzero coefficients  $h[n]$ ,  $n = 0, \pm M, \pm 2M, \dots$ . For filters of this special form, the identity shown in Figure 1.3 holds.

$$\mathbf{x} \longrightarrow \boxed{\downarrow M} \longrightarrow \boxed{H(z)} \longrightarrow \mathbf{y}_1 \quad \equiv \quad \mathbf{x} \longrightarrow \boxed{H(z^M)} \xrightarrow{\mathbf{x}'} \boxed{\downarrow M} \longrightarrow \mathbf{y}_2$$

Figure 1.3: The first noble identity

To show this, note that  $X'(z) = X(z)H(z^M)$  by (1.2.2) implies

$$\begin{aligned} Y_2(z) &= \frac{1}{M} \sum_{k=0}^{M-1} X'(z^{\frac{1}{M}} W_M^k) \\ &= \frac{1}{M} \sum_{k=0}^{M-1} X(z^{\frac{1}{M}} W_M^k) H\left((z^{\frac{1}{M}} W_M^k)^M\right) \\ &= \frac{1}{M} \sum_{k=0}^{M-1} X(z^{\frac{1}{M}} W_M^k) H(z) = Y_1(z). \end{aligned}$$

The second noble identity aims at the interpolation. Suppose this time we want to interpolate a signal  $X(z)$  by a factor of  $L$  and an interpolation filter that has  $L - 1$  zeros between the nonzero coefficients. Then the identity in Figure 1.4 holds since by (1.2.5) we have that

$$Y_2(z) = X'(z)G(z^L) = X(z^L)G(z^L) = Y_1(z).$$



Figure 1.4: The second noble identity

**Polyphase Representation of Systems.** Let  $Q(z)$  be a LTI filter. The decomposition of  $Q(z)$  into a number of  $J$  ( $J \in \mathbb{N}$ ,  $j > 1$ ), i.e., multiple (poly) components of a different delay (phase) is called the polyphase decomposition of  $Q(z)$ . According to the lines of Vaidyanathan [70] we discriminate between two types of this decomposition. The *type I polyphase decomposition* reads

$$Q(z) = \sum_{j=0}^{J-1} z^{-j} Q_j^{\text{p1}}(z^J) \quad (1.2.7)$$

with

$$Q_j^{\text{p1}}(z) = \sum_{n \in \mathbb{Z}} q[Jn + j] z^{-n}.$$

The *type II polyphase decomposition* uses a slightly modified decomposition and is given by

$$Q(z) = \sum_{j=0}^{J-1} z^{-(J-1-j)} Q_j^{\text{p2}}(z^J) \quad (1.2.8)$$

with

$$Q_j^{p2}(z) = Q_{J-1-j}^{p1}(z).$$

For our further discussions is important to see that the polyphase components of the filters in (1.2.7) and (1.2.8) have the form needed for applying the noble identities. Thus we may apply downsampling before filtering when using the polyphase components of the decimation filters and the first noble identity for decimators. Equivalently, by the application of the second noble identity to the polyphase components of an interpolation filter, we can do the upsampling after the filtering for interpolators. We will use these facts for the efficient polyphase implementation of two-channel filter banks in Section 1.3.2.

## 1.3 Two-Channel Filter Banks

Two-channel filter banks consist of an analysis bank and a synthesis bank which decompose an input signal into two subbands. In general, we have a low frequency and high frequency signal which sampling rate is reduced by the analysis bank. The synthesis bank reconstructs these subbands to obtain a common output signal.

### 1.3.1 Critical Sampling and Perfect Reconstruction

Two-channel filter banks allowing a perfect reconstruction of the input signal will be investigated in this section. We will see that they are schemes of decimators and interpolators with appropriately designed filters. For this, let  $H_0(z)$  and  $G_0(z)$  be ideal lowpass filters such that

$$H_0(e^{i\omega}) = \frac{1}{2}G_0(e^{i\omega}) = \begin{cases} 1 & \text{for } 0 \leq |\omega| < \pi/2 \\ 0 & \text{for } \pi/2 \leq |\omega| < \pi. \end{cases}$$

Let further  $H_1(z)$  and  $G_1(z)$  be ideal highpass filters which are modulated version of the filters above such that

$$H_1(e^{i\omega}) = H_0(e^{i(\omega-\pi)}) = \frac{1}{2}G_1(e^{i\omega}) = \frac{1}{2}G_0(e^{i(\omega-\pi)}) = \begin{cases} 0 & \text{for } 0 \leq |\omega| < \pi/2 \\ 1 & \text{for } \pi/2 \leq |\omega| < \pi. \end{cases}$$

The magnitude response of the filters  $H_0(z)$  and  $H_1(z)$  is shown in Figure 1.6 (top). Assume the filters  $H_0(z)$  and  $H_1(z)$  are the decimation filters of 2-fold decimators

whereas  $G_0(z)$  and  $G_1(z)$  are the interpolation filters of 2-fold interpolators. If we arrange these systems as in Figure 1.5 we obtain a two-channel filter bank. The filters  $H_0(z)$  and  $H_1(z)$  are called *analysis filters* and  $G_0(z)$  and  $G_1(z)$  are known as *synthesis filters*.

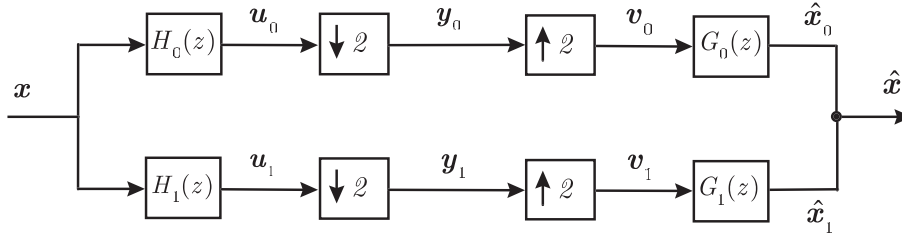


Figure 1.5: Two-channel filter bank with critical sampling

Note that the subbands of such a filter bank have an absolute bandwidth of  $\pi/2$ . From Section 1.2.1 we know that downsampling by a factor of two is the limit here when dealing with aliasing free systems. Therefore, such filter banks are called *critically sampled filter banks* or *maximally decimated filter banks*. The corresponding spectra of the signals in Figure 1.5 are shown symbolically in Figure 1.6 for a given input signal  $X(e^{i\omega})$ . Note that the relation between the spectra can be derived by (1.2.2) and (1.2.5), respectively, on the unit circle. The described effects of bandwidth reduction before downsampling and the removing of the images are noticeable. We see how decimators and interpolators work together to obtain perfect reconstruction.

Clearly, in practice we cannot realize noncausal ideal filters with infinite impulse response. A straightforward approach to cope with this problem is to design filters with narrow transition widths such that the affection of aliasing is low. However, this results in very expensive filter systems. Therefore, one goes another way. We permit aliasing and try to design synthesis filters which compensate it.

From Figure 1.5 we have that  $U_i(z) = H_i(z)X(z)$  which by (1.2.2) yields

$$Y_i(z) = \frac{1}{2} \left( U_i(z^{\frac{1}{2}}) + U_i(-z^{\frac{1}{2}}) \right), \quad i = 0, 1.$$

Using this relation and (1.2.5) we have that

$$\begin{aligned} V_i(z) &= Y_i(z^2) \\ &= \frac{1}{2} (U_i(z) + U_i(-z)) \\ &= \frac{1}{2} (H_i(z)X(z) + H_i(-z)X(-z)), \quad i = 0, 1. \end{aligned}$$

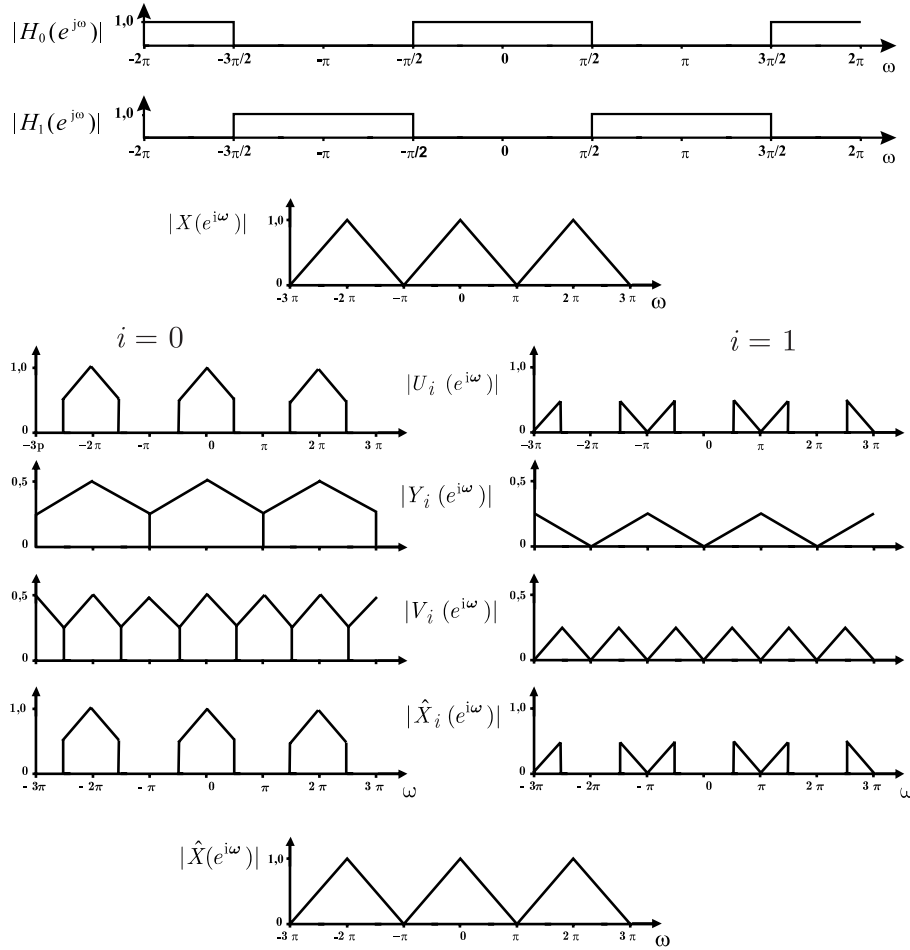


Figure 1.6: The operation of a two-channel filter bank in the frequency domain using ideal filters. The lowpass channel is denoted with  $i = 0$  and highpass channel with  $i = 1$ . The magnitude response of the ideal analysis filters is shown at the top.

From Figure 1.5 we have finally that  $\hat{X}(z) = \hat{X}_0(z) + \hat{X}_1(z) = V_0(z)G_0(z) + V_1(z)G_1(z)$  which with the relation above yields

$$\hat{X}(z) = \frac{1}{2} \underbrace{(H_0(z)G_0(z) + H_1(z)G_1(z))}_{T(z)} X(z) + \frac{1}{2} \underbrace{(H_0(-z)G_0(z) + H_1(-z)G_1(z))}_{A(z)} X(-z). \tag{1.3.9}$$

**Perfect Reconstruction.** The term  $T(z)$  is the LTI transfer function of the filter bank. The term  $A(z)$  stems from the alias component  $U(-z^{\frac{1}{2}})$ , see Section 1.2.1, in our derivation above and represents the aliasing of the filter bank. If  $A(z) = 0$  we

obtain a LTI filter bank although it involves the linear time-variant downsamples and upsamplers. If we further have that  $T(z) = cz^{-l}$ , ( $c \in \mathbb{R}_{>0}$ ,  $l \in \mathbb{Z}$ ) we find that  $\hat{X}(z) = 0.5cz^{-l}X(z)$ . In this case, we obtain a filter bank which output signal is an exact replica of the input signal up to a shift in time and an amplitude factor. Such a filter bank is called a *perfect reconstruction filter bank*. In our following discussions, we restrict the term perfect construction directly to filter banks without amplitude affection, i.e.,  $c = 2$ . By introducing the notation

$$\mathbf{H}_{\text{mod}}(z) = \begin{bmatrix} H_0(z) & H_0(-z) \\ H_1(z) & H_1(-z) \end{bmatrix}, \quad \mathbf{G}_{\text{mod}}(z) = \begin{bmatrix} G_0(z) & G_1(z) \\ G_0(-z) & G_1(-z) \end{bmatrix},$$

the input output relation in (1.3.9) reads

$$\begin{bmatrix} \hat{X}(z) \\ \hat{X}(-z) \end{bmatrix} = \frac{1}{2} \mathbf{G}_{\text{mod}}(z) \mathbf{H}_{\text{mod}}(z) \begin{bmatrix} X(z) \\ X(-z) \end{bmatrix}.$$

Thus, letting  $\mathbf{I}_2$  a  $2 \times 2$  identity matrix, the condition for perfect reconstruction without delay reads

$$\mathbf{G}_{\text{mod}}(z) \mathbf{H}_{\text{mod}}(z) = 2\mathbf{I}_2. \quad (1.3.10)$$

Here  $\mathbf{H}(z)$  and  $\mathbf{G}(z)$  are called the *modulation matrix* of the analysis bank and synthesis bank, respectively.

### 1.3.2 Polyphase Implementation

We decompose the analysis filters into their polyphase components of type I by

$$H_0(z) = H_{00}^{\text{p1}}(z^2) + z^{-1}H_{01}^{\text{p1}}(z^2) \quad (1.3.11)$$

and

$$H_1(z) = H_{10}^{\text{p1}}(z^2) + z^{-1}H_{11}^{\text{p1}}(z^2). \quad (1.3.12)$$

If we now further decompose the synthesis filters into polyphase components of type II, i.e.,

$$G_0(z) = z^{-1}G_{00}^{\text{p2}}(z^2) + G_{01}^{\text{p2}}(z^2)$$

and

$$G_1(z) = z^{-1}G_{10}^{\text{p2}}(z^2) + G_{11}^{\text{p2}}(z^2),$$

and apply the first noble identity (Figure 1.3) for the analysis filters and second noble identity (Figure 1.4) for the synthesis filters we obtain the efficient polyphase implementation of a two-channel filter bank shown in Figure 1.7. Here the downsampling is applied before filtering in the analysis bank and the upsampling comes after filtering in the synthesis bank.

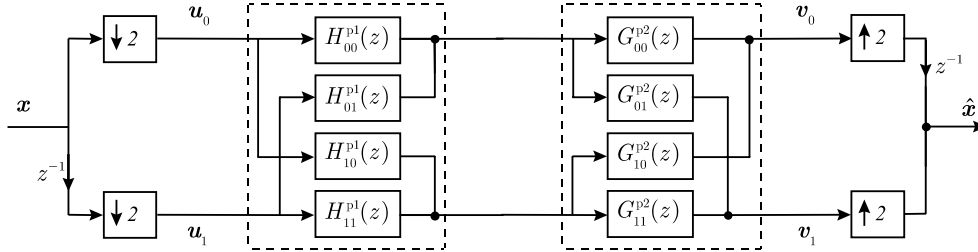


Figure 1.7: Polyphase implementation of a two-channel critically sampled filter bank.

Let us define the *polyphase matrix* of the analysis bank  $\mathbf{H}_{\text{pol}}(z)$  by

$$\mathbf{H}_{\text{pol}}(z) = \begin{bmatrix} H_{00}^{p1}(z) & H_{01}^{p1}(z) \\ H_{10}^{p1}(z) & H_{11}^{p1}(z) \end{bmatrix}$$

and the polyphase matrix of the synthesis bank by

$$\mathbf{G}_{\text{pol}}(z) = \begin{bmatrix} G_{00}^{p2}(z) & G_{10}^{p2}(z) \\ G_{01}^{p2}(z) & G_{11}^{p2}(z) \end{bmatrix}.$$

Then using the signal notation in Figure 1.7 we obtain

$$\begin{bmatrix} V_0(z) \\ V_1(z) \end{bmatrix} = \mathbf{G}_{\text{pol}}(z)\mathbf{H}_{\text{pol}}(z) \begin{bmatrix} U_0(z) \\ U_1(z) \end{bmatrix}.$$

If we have that

$$\mathbf{G}_{\text{pol}}(z)\mathbf{H}_{\text{pol}}(z) = \mathbf{I}_2, \quad (1.3.13)$$

we can remove the decimation and interpolation filters from the filter bank. Since the remaining scheme of delays, downsamplers, and upsamplers produces only a delay, (1.3.13) becomes the condition for a perfect reconstruction filter bank. When dealing with causal systems, we have an additional delay in (1.3.13) such that  $\mathbf{G}_{\text{pol}}(z)\mathbf{H}_{\text{pol}}(z) = z^{-l}\mathbf{I}_2$ , ( $l \in \mathbb{N}$ ).

By introducing the delay matrix  $\mathbf{D} = \text{diag}[1, z^{-1}]$  and the  $2 \times 2$  discrete Fourier transform matrix  $\mathbf{W}_2 = (W_2^{mn})_{m,n=0}^1$ , we find the relation

$$\mathbf{H}_{\text{mod}}(z) = \mathbf{H}_{\text{pol}}(z^2)\mathbf{D}(z)\mathbf{W}_2 \quad (1.3.14)$$

for the modulation and polyphase matrix of the analysis bank.

### 1.3.3 Paraunitary Filter Banks

Two-channel filter banks which always satisfy the perfect reconstruction requirement are *paraunitary filter banks*. Before introducing these filter banks, let us define the following terms.

**Paraconjugation.** We define the *paraconjugation* of a transfer function  $Q(z)$  by

$$\tilde{Q}(z) = Q_*(z^{-1}).$$

Here all coefficients  $q[\cdot]$  are conjugated and inverted in time, i.e., in time-domain we have that  $\tilde{q}[\cdot] = q^*[-\cdot]$ . Let  $\mathbf{q}$  be a finite impulse response (FIR) filter of order  $N$  with real filter coefficients. Then its paraconjugation is causal if we use an additional delay such that

$$z^{-N}\tilde{Q}(z) = q[N] + z^{-1}q[N-1] + \dots + z^{-N}q[0],$$

which reads in the time-domain as  $\tilde{q}[n] = q[N-n]$  ( $n = 0, 1, \dots, N$ ). Throughout this thesis, the complex conjugation is always negligible since we will only consider real filter coefficients.

**Paraunitary.** We call a matrix  $\mathbf{Q}(z)$  *paraunitary* if

$$\mathbf{Q}^T(z^{-1})\mathbf{Q}(z) = \tilde{\mathbf{Q}}(z)\mathbf{Q}(z) = c\mathbf{I}_2, \quad \forall z, c \in \mathbb{R}_{>0}. \quad (1.3.15)$$

If  $\mathbf{Q}(z)$  is square, we have further that  $\tilde{\tilde{\mathbf{Q}}}(z)\mathbf{Q}(z) = \mathbf{Q}(z)\tilde{\tilde{\mathbf{Q}}}(z)$ . When dealing with complex filters, we have also to conjugate the filter coefficients of  $\mathbf{Q}^T(z^{-1})$ . Note that on the unit circle and  $c = 1$  paraunitary is equivalent to unitary. Note also that a product of paraunitary matrices is also paraunitary. We call a matrix which has  $c = 1$  in (1.3.15) *normalized paraunitary* (NP). If a NP matrix  $\mathbf{Q}(z)$  is FIR, i.e., consists of polynomial entries, and square, then its determinant is a pure delay due to (1.3.15), i.e.,

$$\det \mathbf{Q}(z) = \pm z^{-l}, \quad l \in \mathbb{N}.$$

Of course, given a paraunitary polyphase matrix  $\mathbf{H}_{\text{pol}}(z)$  the choice  $\mathbf{G}_{\text{pol}}(z) = \mathbf{H}_{\text{pol}}^{-1}(z) = \tilde{\mathbf{H}}_{\text{pol}}(z)$  results in a perfect reconstruction system due to (1.3.13). Filter banks with a NP polyphase matrix are called *NP filter banks* in our further discussions.

From (1.3.14) we have that the modulation matrix  $\mathbf{H}_{\text{mod}}(z)$  is paraunitary with

$$\mathbf{H}_{\text{mod}}(z)\tilde{\mathbf{H}}_{\text{mod}}(z) = 2\mathbf{I}_2, \quad (1.3.16)$$

if and only if the polyphase matrix has the form

$$\mathbf{H}_{\text{pol}}(z)\tilde{\mathbf{H}}_{\text{pol}}(z) = \mathbf{I}_2. \quad (1.3.17)$$

**Filter Relation.** When dealing with a causal two-channel NP filter bank with FIR filters of odd order  $N$ , the analysis filters  $H_0(z)$  and  $H_1(z)$  are related as

$$H_1(z) = sz^{-N}\tilde{H}_0(-z), \quad \text{where } s \in \{\pm 1\} \text{ and } N \in \mathbb{N}, N \text{ odd.} \quad (1.3.18)$$

To show this, note that (1.3.16) yields

$$\tilde{\mathbf{H}}_{\text{mod}}(z)\mathbf{H}_{\text{mod}}(z) = 2\mathbf{I}_2,$$

which implies

$$\tilde{H}_0(z)H_0(z) + \tilde{H}_1(z)H_1(z) = 2, \quad (1.3.19)$$

$$H_0(z)\tilde{H}_0(-z) + H_1(z)\tilde{H}_1(-z) = 0. \quad (1.3.20)$$

The filters  $H_0(z)$  and  $H_1(z)$  are coprime. To see this, suppose  $H_0(z)$  and  $H_1(z)$  are not coprime, and call their common factor  $F(z)$  such that  $H_0(z) = F(z)H'_0(z)$  and  $H_1(z) = F(z)H'_1(z)$ . Then (1.3.19) implies that

$$\tilde{F}(z)F(z)(H'_0(z)H'_0(z) + \tilde{H}'_1(z)H'_1(z)) = 2$$

which for all zeros of  $F(z)$  is also zero, contradicting the fact that the right hand side is a constant. Using this finding along with (1.3.20), we see that  $H_1(z)$  must have the form  $H_1(z) = sz^{-N}H_0(-z)$ , where  $N$  is a positive integer which provides the causality of  $H_1(z)$ . Substituting this in (1.3.19) gives  $\tilde{H}_0(z)H_0(z) + s^2H_0(-z)\tilde{H}_0(-z) = 2$  which along with the fact that  $H_0(z)$  is a *power symmetric half band filter*, i.e., it satisfies

$$H_0(z)\tilde{H}_0(z) + H_0(-z)\tilde{H}_0(-z) = 2, \quad (1.3.21)$$

directly yields  $s \in \{\pm 1\}$ . From (1.3.19) we finally see that  $N$  has to be odd.

By  $\mathbf{G}_{\text{mod}}(z) = \tilde{\mathbf{H}}_{\text{mod}}(z)$  the synthesis filters of a paraunitary filter bank are given by

$$G_i(z) = \tilde{H}_i(z), \quad i = 0, 1. \quad (1.3.22)$$

If  $H_0(z)$  and  $H_1(z)$  are analysis filters of order  $N$ , a causal solution for the synthesis filters is given by

$$G_i(z) = z^{-N} \tilde{H}_i(z), \quad i = 0, 1, \quad N \in \mathbb{N}, \quad N \text{ odd}. \quad (1.3.23)$$

Throughout this thesis we set  $s = +1$  in (1.3.18). Note that (1.3.18) and (1.3.23) are exactly the relations which give the well known *Conjugate Quadrature Filters* [56, 57], see also [39]. Sometimes these filters are called *Quadrature Mirror Filters* although this term was much earlier used for filters which only provide an alias free filter bank that still suffers from LTI distortions [9].

## 1.4 Multiresolution Decompositions of $\ell^2$

So far, we have only considered two-channel filter banks. These filter banks are of course of limited applicability. For most applications we are interested in filter banks allowing a more flexible splitting than in only two subbands. But as we will see, such filter banks can easily be constructed using NP two-channel filter banks as building blocks cascaded in trees. Such tree structured filter banks directly lead to the idea of multiresolution analysis and wavelet transforms [10, 36, 76, 59]. In the context of wavelets, multiresolution is in general associated with a decomposition of the Hilbert space of all square integrable functions  $L^2(\mathbb{R})$ . A fast algorithm for a multiresolution analysis of  $L^2(\mathbb{R})$  was introduced in [37] that is based on cascaded NP filter banks with zero mean highpass filter.

Indeed, wavelets are closely related to multirate filter banks and both subjects can be treaded from a common unifying standpoint within the framework of multiresolution decompositions. The choice of an appropriate wavelet basis and the design of suitable filter banks share the same theme: the construction of 'good' bases for signal representations.

**Discrete–Time Approach.** Discrete–time multiresolution and wavelet concepts have been proposed [75, 22, 48] (see also the book of Vetterli & Kovačević [76] and Cohen & Ryan [7]) as a discrete–time pendant of the general wavelet theory. These concepts deal with the decomposition of discrete–time signals into a set of discrete–time wavelets. Accordingly, a wavelet is a sequence  $\mathbf{g}$  with compact support that oscillates around zero such that  $\sum_{n \in \mathbb{Z}} g[n] = 0$  rather than a continuous function in  $L^2(\mathbb{R})$  of zero mean. The discrete–time formalism is straightforward for digital signal processing and will be used exclusively in this thesis. The term discrete–time is left out in the following, unless there is room for confusion. We assume without a word that the highpass filter of the two–channel filter banks has a zero mean such that its impulse response corresponds to a wavelet in our subsequent discussion. As usual, we will stick to the very same two–channel building block on every level of tree structured filter banks (although only the NP property on each level is needed).

### 1.4.1 Orthonormal Expansions via Filter Banks

It is known that NP filter banks provide orthonormal expansions of signals  $\mathbf{x} \in \ell^2$ , see [75, 22, 58] for pioneering papers. For our further discussions, we use the signal and filter notation from Figure 1.5 such that we have two analysis filters  $H_0(z), H_1(z)$ , two synthesis filters  $G_0(z), G_1(z)$ , an input signal  $\mathbf{x}$ , and an output signal  $\hat{\mathbf{x}}$ . The output signals of the analysis bank are denoted by  $\mathbf{y}_0$  and  $\mathbf{y}_1$ , respectively. In contrast to the previous sections, we are only interested in orthonormal expansions by filter banks and not their system theoretical meaning. Therefore, we deal with noncausal systems here which simplifies the notation. We assume that our filter bank is NP and produces no delay.

Let  $U(z)$  and  $V(z)$  be LTI filters. Then the relation  $U(z)\tilde{V}(z) + U(-z)\tilde{V}(-z) = c$  ( $c \in \mathbb{R}$ ) in the time–domain reads

$$\sum_{n \in \mathbb{Z}} u[n]v[n - k] + (-1)^k \sum_{n \in \mathbb{Z}} u[n]v[n - k] = c\delta[k], \quad k \in \mathbb{Z}.$$

Using this finding and the fact that (1.3.16) and (1.3.22) implies

$$\begin{aligned} G_0(z)\tilde{G}_0(z) + G_0(-z)\tilde{G}_0(-z) &= 2, \\ G_1(z)\tilde{G}_1(z) + G_1(-z)\tilde{G}_1(-z) &= 2, \\ G_0(z)\tilde{G}_1(z) + G_0(-z)\tilde{G}_1(-z) &= 0, \end{aligned}$$

we obtain the following time-domain relations for a NP two-channel filter bank

$$\begin{aligned}\sum_{n \in \mathbb{Z}} g_0[n]g_0[n - 2k] &= \delta[k], \\ \sum_{n \in \mathbb{Z}} g_1[n]g_1[n - 2k] &= \delta[k], \\ \sum_{n \in \mathbb{Z}} g_0[n]g_1[n - 2k] &= 0,\end{aligned}$$

for  $k \in \mathbb{Z}$ . Thus the impulse responses of a two-channel NP synthesis filter bank form an orthonormal set by their even shifts. From Figure 1.5 a sequence  $\mathbf{x} \in \ell^2$  has the representation  $\hat{\mathbf{x}} = \mathbf{x} = \hat{\mathbf{x}}_0 + \hat{\mathbf{x}}_1$ . The expansions of  $\hat{\mathbf{x}}_0$  and  $\hat{\mathbf{x}}_1$  are given by (1.2.6) with expansion coefficients  $\mathbf{y}_k$  ( $k = 0, 1$ ) in Figure 1.5 due to (1.2.3). More precisely, we have that

$$\begin{aligned}x[n] &= \hat{x}_0[n] + \hat{x}_1[n] \\ &= \sum_{m \in \mathbb{Z}} y_0[m]g_0[n - 2m] + \sum_{m \in \mathbb{Z}} y_1[m]g_1[n - 2m] \\ &= \sum_{m \in \mathbb{Z}} \left( \sum_{i \in \mathbb{Z}} x[i]h_0[2m - i] \right) g_0[n - 2m] \\ &\quad + \sum_{m \in \mathbb{Z}} \left( \sum_{i \in \mathbb{Z}} x[i]h_1[2m - i] \right) g_1[n - 2m].\end{aligned}$$

Thus when noting that (1.3.22) implies  $h_k[\cdot] = g_k[-\cdot]$  ( $k = 0, 1$ ), this can be rewritten as

$$\begin{aligned}x[n] &= \sum_{m \in \mathbb{Z}} \langle x[\cdot], g_0[\cdot - 2m] \rangle_{\ell^2} g_0[n - 2m] \\ &\quad + \sum_{m \in \mathbb{Z}} \langle x[\cdot], g_1[\cdot - 2m] \rangle_{\ell^2} g_1[n - 2m]\end{aligned}\tag{1.4.24}$$

and the set  $\{g_0[\cdot - 2m], g_1[\cdot - 2m] : m \in \mathbb{Z}\}$  constitutes an orthonormal basis for  $\ell^2$ . The signal splitting above is important for our further discussions since the subsequent orthonormality relations follow simply by induction of this concept.

### 1.4.2 Octave-Band Decomposition

We are often interested in filter banks which decompose a given signal  $\mathbf{x}$  into multiple subbands of different bandwidths. The most popular representative of such filter banks

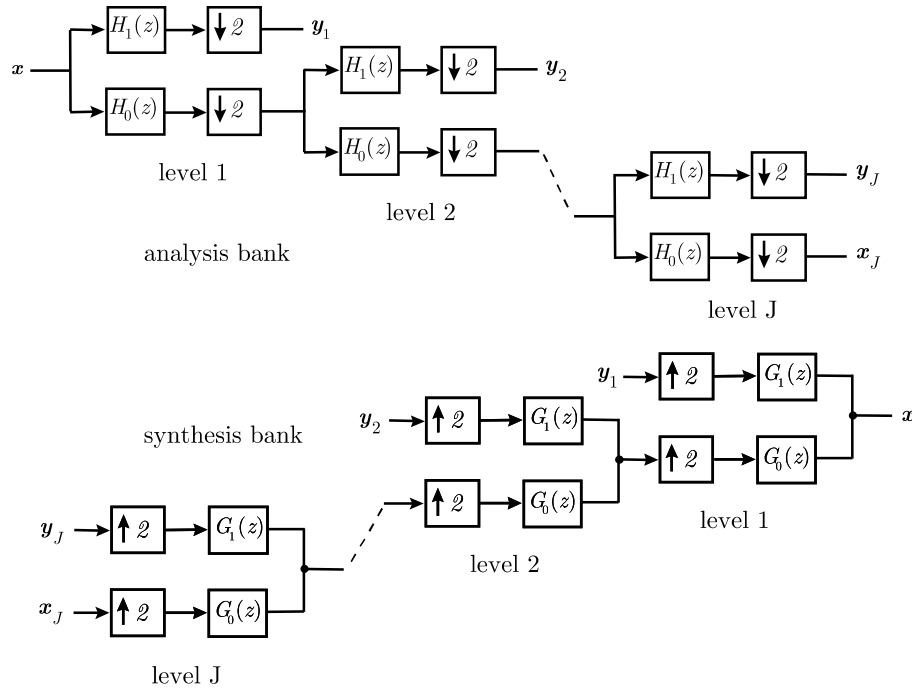


Figure 1.8: Analysis and synthesis bank of an octave-band tree.

is the octave-band tree. The corresponding octave-band or logarithmic spectrum is very natural for various fields of signal processing, e.g., in biomedical signal processing [4]. An octave-band filter bank is shown in Figure 1.8.

By the first and second noble identity, see Section 1.2.3, we obtain the relation in Figure 1.9 (top) for the analysis bank and in Figure 1.9 (bottom) for the synthesis bank, respectively, of the octave-band tree. That is, we have separated the LTI filters from the multirate operations. Applying these relations successively on the tree shown in Figure 1.8 we obtain the scheme in Figure 1.10. This scheme is called the *equivalent parallel structure* of the octave-band tree, or more generally, a *parallel structured filter bank*. It is easy to check that the synthesis filters on level  $j = 1, \dots, J$  in Figure 1.10 are given by

$$Q_{j,1}(z) = G_1(z^{2^{j-1}}) \prod_{m=0}^{j-2} G_0(z^{2^m}), \quad (1.4.25)$$

$$Q_{j,0}(z) = \prod_{m=0}^{j-1} G_0(z^{2^m}), \quad (1.4.26)$$

and the analysis filters are the paraconjugate of these filters.

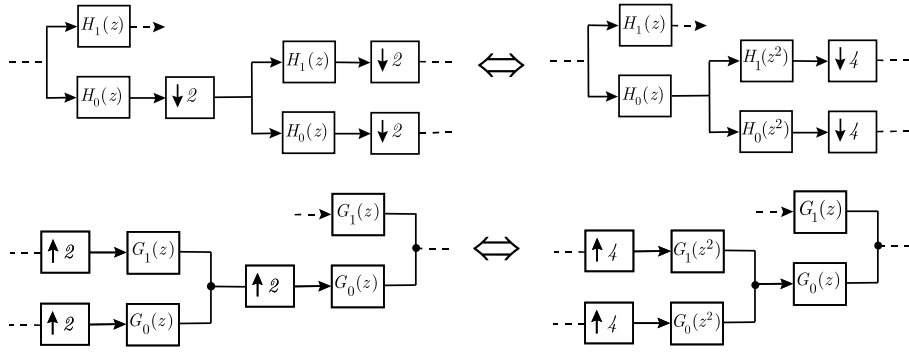


Figure 1.9: Equalities for an analysis (top) and synthesis (bottom) filter bank tree.

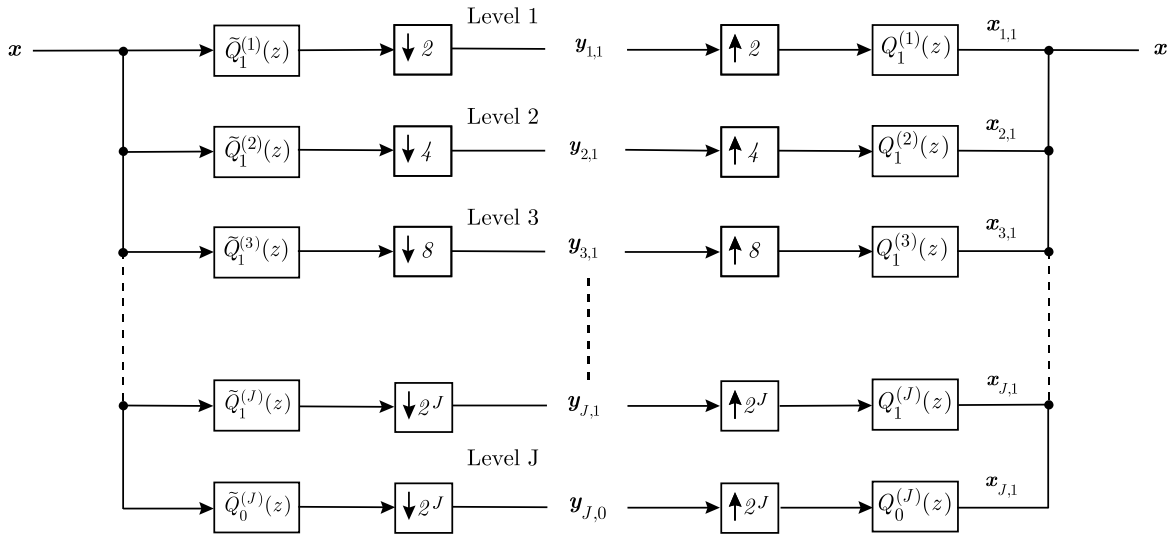


Figure 1.10: The equivalent parallel structure of the octave-band tree.

Hence with appropriate sampling the filters  $\tilde{Q}_{j,k}(z)$  ( $k = 0, 1$ ) bring you from the original signal  $\mathbf{x}$  to the subband of level  $j$  without recursively applying  $H_0(z)$  and  $H_1(z)$ . Analogously, the filters  $Q_{j,k}(z)$  ( $k = 0, 1$ ) reconstruct each subband from level  $j$ . Now we have a simple scheme of  $2^j$ -fold decimators and interpolators ( $j = 1, \dots, J$ ). Note that due to (1.4.25) and (1.4.26) the order of the filters on level  $j$  is given by  $N^{(j)} = (2^j - 1)N$  when dealing with FIR filters  $G_0(z)$  and  $G_1(z)$  of order  $N$  in the NP building blocks. Let  $\mathbf{q}_{j,k}^m = (q_{j,k}[n - 2^j m])_{n \in \mathbb{Z}}$  ( $k = 0, 1$ ) denote the translation of  $\mathbf{q}_{j,k}$  by  $2^j m$  samples. Due to the NP property of each two-channel building block, the

impulse responses of the filters in (1.4.25) and (1.4.26) satisfy

$$\langle \mathbf{q}_{j,0}^0, \mathbf{q}_{j,0}^m \rangle_{\ell^2} = \delta[m], \quad (1.4.27)$$

$$\langle \mathbf{q}_{i,1}^m, \mathbf{q}_{j,1}^n \rangle_{\ell^2} = \delta[i-j]\delta[m-n], \quad (1.4.28)$$

$$\langle \mathbf{q}_{j,0}^0, \mathbf{q}_{j,1}^m \rangle_{\ell^2} = 0, \quad (1.4.29)$$

$m, n \in \mathbb{Z}$ ,  $i, j = 1, \dots, J$ .

In direct analogy to Section 1.4.1, we may obtain all the signals of the parallel structured filter bank in Figure 1.10 by  $2^j$ -fold decimators and interpolators. In other words, the reconstructed subbands  $\mathbf{x}_j$  ( $j = 1, \dots, J$ ) are given by (1.2.6) such that  $\mathbf{x}_j = \sum_{m \in \mathbb{Z}} y_{j,k}[m] \mathbf{q}_{j,k}^m$ . Using (1.2.3), the expansion coefficients (subbands) are given  $y_{j,k}[m] = \langle \mathbf{x}, \mathbf{q}_{j,k}^m \rangle_{\ell^2}$  when noting that the analysis filters are the paraconjugated synthesis filters.

**Multiresolution Analysis.** We can formalize the decomposition by octave-band filter banks to a multiresolution analysis of  $\ell^2$ . For this, we introduce the spaces  $\Omega_{0,0} = \ell^2$  and

$$\Omega_{j,0} = \overline{\text{span}\{\mathbf{q}_{j,0}^m : m \in \mathbb{Z}\}}, \quad \Omega_{j,1} = \overline{\text{span}\{\mathbf{q}_{j,1}^m : m \in \mathbb{Z}\}}.$$

Note that  $\{\mathbf{q}_{j,k}^m : m \in \mathbb{Z}\}$  forms an orthonormal basis of  $\Omega_{j,i}$  ( $k = 0, 1$ ). Further we have by (1.4.26) the multiresolution structure  $\Omega_{J,0} \subset \dots \subset \Omega_{2,0} \subset \Omega_{1,0} \subset \Omega_{0,0}$  and by (1.4.29) that

$$\Omega_{j-1,0} = \Omega_{j,0} \oplus \Omega_{j,1}, \quad (1.4.30)$$

where  $\oplus$  denotes the orthogonal sum. Thus the space  $\ell^2$  can be decomposed as  $\ell^2 = \Omega_{J,0} \oplus \bigoplus_{j=1}^J \Omega_{j,1}$  and the set

$$\{\mathbf{q}_{J,0}^m, \mathbf{q}_{j,1}^m : j = 1, \dots, J; m \in \mathbb{Z}\} \quad (1.4.31)$$

constitutes an orthonormal basis for  $\ell^2$ .

The basis functions  $\mathbf{q}_{j,k}$  have a compact support when using FIR filters. Thus the coefficients  $\mathbf{y}_{j,k}$  ( $k = 0, 1$ ) allow for a representation of features being local in time. Note that the support of the basis functions increases with  $j$  due to (1.4.25) and (1.4.26). From (1.4.30) we have further that  $\Omega_{i,1} \perp \Omega_{j,1}$  for  $i \neq j$ . Therefore, the subbands carry non-redundant information of  $\mathbf{x}$  with a resolution matched to a particular level  $j$ . Since we are dealing with orthonormal expansions, the *Parseval identity* holds for the individual subbands on level  $j$  ( $j = 1, \dots, J$ ) and their reconstructions, i.e.,  $\|\mathbf{x}_{j,k}\|_{\ell^2}^2 = \|\mathbf{y}_{j,k}\|_{\ell^2}^2$  ( $k = 0, 1$ ).

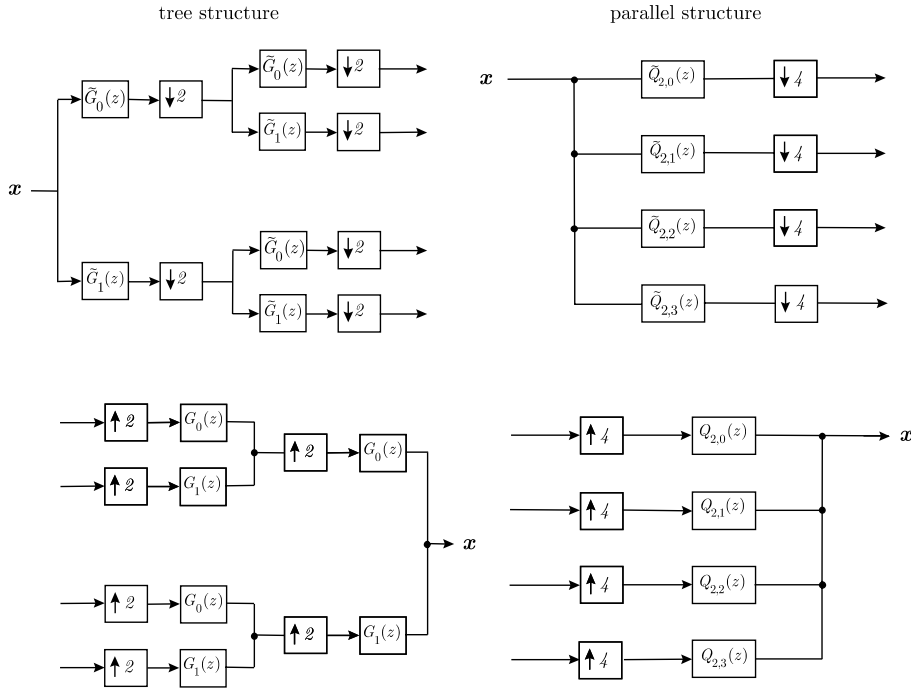


Figure 1.11: Uniform band filter bank in tree structure and parallel structure: analysis bank (top) and synthesis bank (bottom).

### 1.4.3 Generalized Binary Tree Decompositions

Clearly, the concept above can easily be extended to an arbitrary tree structured filter bank, where the space  $\Omega_{0,0}$  is decomposed into a more general structure of mutually orthogonal subspaces by the two-channel NP building blocks such that

$$\Omega_{j,k} = \Omega_{j+1,2k} \oplus \Omega_{j+1,2k+1} \quad (1.4.32)$$

for  $j = 0, 1, \dots, J$ ,  $k = 0, 1, \dots, 2^j - 1$ . Such binary trees can ever be expressed by their equivalent parallel structures when using the relations in Figure 1.9. For a given pair  $(j, k) \in \{1, \dots, J\} \times \{0, 1, \dots, 2^j - 1\}$ , let us denote the filters of the equivalent parallel structure by  $Q_{j,k}(z)$ . For the translation of their impulse response by  $2^j m$  samples we use again the notation  $\mathbf{q}_{j,k}^m$ . Suppose our aim is to decompose a signal in  $J$  subbands with equal bandwidth by NP two-channel building blocks with synthesis filters  $G_0(z)$  and  $G_1(z)$ . Then we have a fixed  $J$  with filters  $Q_{J,k}(z)$ ,  $k = 0, 1, \dots, J - 1$  and the set

$$\{\mathbf{q}_{J,k}^m : k = 0, 1, \dots, 2^J - 1, m \in \mathbb{Z}\}$$

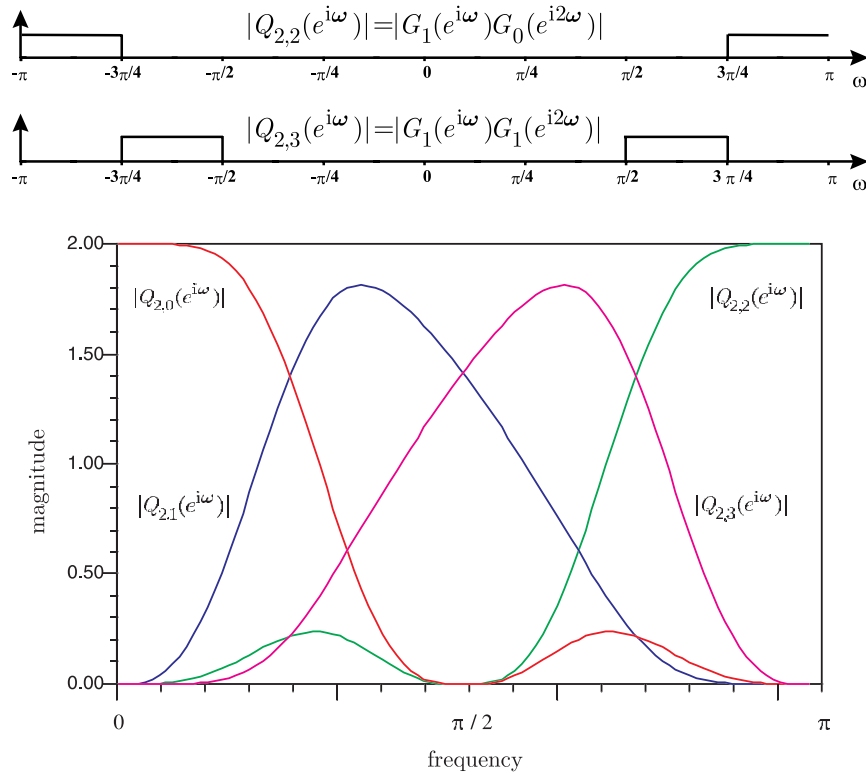


Figure 1.12: The magnitude response of a uniform band synthesis bank with two-channel building blocks (with filters  $G_0(z)$  and  $G_1(z)$ ) and decomposition depth  $J = 2$ . For ideal filters  $G_0(z)$  and  $G_1(z)$  the magnitude of  $Q_{2,2}(z)$  and  $Q_{2,3}(z)$  is shown at the top. The magnitude response of the whole synthesis bank for 'real filters' is depicted at the bottom.

constitutes an orthonormal basis for  $\Omega_{0,0}$  due to the paraunitarity of the two-channel building blocks. Decompositions of this kind are called *uniform band decompositions* and are realized by *uniform band filter banks*.

For instance, if  $J = 2$  we obtain the tree structure and parallel structure of the filter bank which is shown in Figure 1.11. By the relations in Figure 1.9, we have that  $Q_{2,0}(z) = G_0(z)G_0(z^2)$ ,  $Q_{2,1}(z) = G_0(z)G_1(z^2)$ ,  $Q_{2,2}(z) = G_1(z)G_0(z^2)$ , and  $Q_{2,3}(z) = G_1(z)G_1(z^2)$ . The magnitude response of these filters is shown in Figure 1.12 using ideal (top, only  $Q_{2,2}(z)$  and  $Q_{2,3}(z)$ ) and 'real' filters (bottom)  $G_0(z)$  and  $G_1(z)$ .

**Wavelet Packet Decomposition.** Decompositions by an arbitrary binary tree structure are called *wavelet packet decompositions*, see [8, 81] for details. Let  $\mathbf{x}$  be the input sequence of an arbitrary binary tree structured filter bank consisting of two-channel

NP building blocks. Let us define the projection operator

$$P_{j,k} : \Omega_{0,0} \longrightarrow \Omega_{j,k}, \quad j = 1, \dots, J, \quad k = 0, \dots, 2^j - 1$$

with

$$P_{j,k} \mathbf{x} = \sum_{m \in \mathbb{Z}} y_{j,k}[m] \mathbf{q}_{j,k}^m. \quad (1.4.33)$$

The expansion coefficients are given by

$$y_{j,k}[m] = \langle \mathbf{x}, \mathbf{q}_{j,k}^m \rangle_{\ell^2}. \quad (1.4.34)$$

Note that this expansion stems directly from (1.2.3) and (1.2.6) applied to the parallel structure of binary trees.

Since octave-band decompositions are simply a special case of the wavelet packet decompositions, we do not strictly distinguish between them in this thesis and call these methods in a generalized manner multiresolution or wavelet decompositions. Note that not all basis functions of the tree are offset free, i.e., have a zero mean, and correspond to wavelets. We call them in a generalized manner *atoms* or more precisely, *time-scale atoms* since they are localized in time and scale. Note also that even in the case of uniform band decompositions an increasing index  $k$  does not necessarily correspond to higher frequency atoms (due to the periodicity of the filters) as one would expect. In the context of wavelet packets, this fact underlies the so-called *Paley ordered* [81] wavelet packet tree and is noticeable in Figure 1.12. Of course, for representing a signal  $\mathbf{x} \in \Omega_{0,0}$ , the tree of a uniform band decomposition has redundant subspaces  $\Omega_{j,k}$ , ( $j = 1, \dots, J$ ,  $k = 0, \dots, 2^j - 1$ ). Given a decomposition depth  $J$ , we will call all the orthonormal bases associated with a uniform band binary tree a *dictionary* of orthonormal bases. A collection of dictionaries is called a *library*. Thus we select the dictionary from a library. It goes without saying that a dictionary is defined by a two-channel NP building block.

**Finite Length Signals.** When dealing with finite length signals, i.e., sample blocks  $\mathbf{x} \in \Omega_{0,0} \subset \mathbb{R}^d$ , we use the *wraparound technique* [46, 59] throughout this thesis. The signals analyzed in our applications are highly correlated at their boundary points and thus this technique does not lead to any serious distortions. We will also exclusively deal with signals which dimension  $d$  is a power of 2. With respect to the downsampling

operation, we define a maximal decomposition depth by  $J_{\max} = \log_2 d$ . For a fixed level  $j$  and maximal decomposition depth of  $J_{\max}$ , we define the set of indices

$$\mathcal{T}_j = \{0, 1, \dots, 2^{J_{\max}-j} - 1\}.$$

Each subspace  $\Omega_{j,k}$ , ( $j = 1, \dots, J$ ,  $k = 0, \dots, 2^j - 1$ ) is spanned by the translations of the corresponding atom  $\mathbf{q}_{j,1}^m$  with  $m \in \mathcal{T}_j$  in the case of a block decomposition. Note also that we have the standard Euclidean basis in  $\mathbb{R}^d$  for  $j = 0$ .

## 1.5 Signal-Adapted Filter Banks

A general issue when applying wavelet decompositions is the design of an appropriate NP building block. We can roughly distinguish between three approaches to filter bank design. The first and classical procedure is to design frequency selective filters. The second approach has arisen with the development of wavelet theory and aims at the design of very smooth or regular filters, see Section 1.5.1.

The third approach consists in the design of signal-adapted perfect reconstruction filter banks by means of *energy compaction* as approach to optimal subband coding and is an active field of research, see [24, 12, 1, 68, 41, 42, 71, 34, 5] and [72] for a very recent review article. Here the design aims at energy compaction and coding gain [25] maximization, respectively, often formulated as multistage optimization problem (for a binary tree this means that we use distinct two-channel NP building blocks in the tree). The solution has to satisfy the so-called *principal component property* [5], i.e., a minimization of the mean-square error caused by reconstruction after dropping a given number of subbands with the lowest variance, sometimes called *the weakest subbands*.

For filter banks which satisfy the conditions derived earlier for implementing wavelet expansions, this corresponds to the design of optimal orthonormal wavelets for signal compression, see [67, 68, 54] for a separated and somewhat independent treatment of wavelets. Clearly, such compaction filters are closely related to the *Karhunen-Loève transform* [24, 79, 2, 3, 50], see also Section ??, and for a FIR uniform band filter bank with  $J$  bands where the order of the filters is restricted to be less than  $J$ , the optimal solution is the *Karhunen-Loève Coder* [34].

### 1.5.1 Lattice Structure Based Filter Banks

In the initial paper of Delsarte et al. [12] on signal-adapted filter banks with multiresolution architecture, the *lattice structure* was utilized for a multistage coding gain maximization as efficient approximation of the Karhunen–Loève transform. Here significant improvements were observed in contrast to non-adapted implementations for image compression. In recent studies, we have shown that an adaptation based on lattice structure and appropriate class separability criteria is an effective tool for real world pattern recognition tasks in various settings [28, 29, 28, 26, 27, 30, 31, 32, 26, 62, 60, 61, 63, 65, 64]. Although the theory of signal-adapted filter banks is more sophisticated nowadays as in [12], e.g., see [41, 42] for a first globally optimal solution with constraint filter lengths and [5] for a state of the art report, we rely on the lattice structure which is well suited for our purpose. It provides a very efficient parameterization and can even be applied in settings where the objective function seems not to allow for sophisticated calculus based optimization strategies – as for applications in machine learning we have in mind.

**Lattice Decomposition.** In our further discussions, we follow the lines of Vaidyanathan & Hoang [73, 70] and Strang & Nguyen [59]. Let  $\mathbf{H}_{\text{pol}}(z)$  be the NP polyphase matrix of the analysis filter bank consisting of real FIR filters  $H_0(z)$  and  $H_1(z)$  of order  $2K + 1$ . We introduce the *Givens rotation* [19] that is defined as

$$\mathbf{R}(\vartheta) = \begin{bmatrix} \cos \vartheta & \sin \vartheta \\ -\sin \vartheta & \cos \vartheta \end{bmatrix}.$$

We show that  $\mathbf{H}_{\text{pol}}(z)$  has always a decomposition of the form

$$\mathbf{H}_{\text{pol}}(z) = \left( \prod_{i=0}^{K-1} \mathbf{R}(\vartheta_i) \mathbf{D}(z) \right) \mathbf{R}(\vartheta_K), \quad (1.5.35)$$

where  $\vartheta_K \in [0, 2\pi[$ ,  $\vartheta_i \in [0, \pi[$  ( $i = 0, \dots, K - 1$ ). For this purpose, we introduce the matrices

$$\Theta_i = \begin{bmatrix} h_0[2i] & h_0[2i + 1] \\ h_1[2i] & h_1[2i + 1] \end{bmatrix}, \quad i = 0, 1, \dots, K.$$

Then we can express the polyphase matrix as

$$\mathbf{H}_{\text{pol}}^K(z) = \sum_{i=0}^K \Theta_i z^{-i}. \quad (1.5.36)$$

The superscript  $K$  of the polyphase matrix will become clear later. Substituting (1.5.36) in (1.3.15) we find

$$\sum_{i=0}^K \Theta_i^T \Theta_{i+m} = \mathbf{I}_2 \delta[m]$$

which implies that  $\Theta_0^T \Theta_K = \mathbf{0}$ . Thus  $\Theta_0$  and  $\Theta_K$  are singular matrices so that there exists a real nonzero vector  $\mathbf{u} = (\sin \vartheta_K, \cos \vartheta_K)^T$  ( $\vartheta_K \in [0, \pi[$ ) such that

$$\mathbf{u}^T \Theta_0 = \mathbf{0}. \quad (1.5.37)$$

Now we consider the product  $\mathbf{R}^T(\vartheta_0) \mathbf{H}_{\text{pol}}^K(z)$  which we can express as

$$\begin{bmatrix} \cos \vartheta_0 & -\sin \vartheta_0 \\ \sin \vartheta_0 & \cos \vartheta_0 \end{bmatrix} \sum_{i=0}^K \Theta_i z^{-i}. \quad (1.5.38)$$

By (1.5.37) this product can be rewritten as

$$\mathbf{R}^T(\vartheta_0) \mathbf{H}_{\text{pol}}^K(z) = \mathbf{D}(z) \mathbf{H}_{\text{pol}}^{K-1}(z)$$

and thus

$$\mathbf{H}_{\text{pol}}^K(z) = \mathbf{R}(\vartheta_0) \mathbf{D}(z) \mathbf{H}_{\text{pol}}^{K-1}(z). \quad (1.5.39)$$

Here  $\mathbf{H}_{\text{pol}}^{K-1}(z)$  has a reduced degree in the sense that  $\det \mathbf{H}_{\text{pol}}^{K-1}(z) = z \cdot \det \mathbf{H}_{\text{pol}}^K(z)$ . It is easy to check that  $\mathbf{H}_{\text{pol}}^{K-1}(z)$  is also NP since we have that  $\tilde{\mathbf{H}}_{\text{pol}}^K(z) \mathbf{H}_{\text{pol}}^K(z) = \tilde{\mathbf{H}}_{\text{pol}}^{K-1}(z) \mathbf{H}_{\text{pol}}^{K-1}(z)$  due to the orthogonality of  $\mathbf{R}(\vartheta_k)$  and paraunitarity of  $\mathbf{D}(z)$ . Hence we have extracted a NP building block of degree one to reduce the degree of  $\mathbf{H}_{\text{pol}}^K(z)$ . Applying this reduction  $K$  times, we arrive at a constant orthogonal matrix  $\mathbf{H}_{\text{pol}}^0(z)|_{z=1}$  with determinant  $\pm 1$  where we assume a positive sign in the following, i.e.,  $\det \mathbf{H}_{\text{pol}}^0(z)|_{z=1} = 1$ . Clearly, we can express the orthogonal matrix  $\mathbf{H}_{\text{pol}}^0(z)|_{z=1}$  by the Givens rotation such that  $\mathbf{H}_{\text{pol}}^0(z)|_{z=1} = \mathbf{R}(\vartheta_K)$  ( $\vartheta_K \in [0, 2\pi[$ ). Summarizing these facts, we conclude that  $\mathbf{H}_{\text{pol}}^K(z)$  has always a lattice decomposition of the form (1.5.35).

The polyphase implementation by the lattice structure is shown in Figure 1.13. Note that we have simply replaced the LTI filters in Figure 1.7 by the lattice structure to obtain Figure 1.13.

**Highpass with Zero Mean.** For most application we wish to consider highpass filters that have a zero mean, i.e.,  $H_1(z)|_{z=1} = 0$ , which is also the necessary condition for implementing wavelet decompositions in the sense of our earlier discussions.

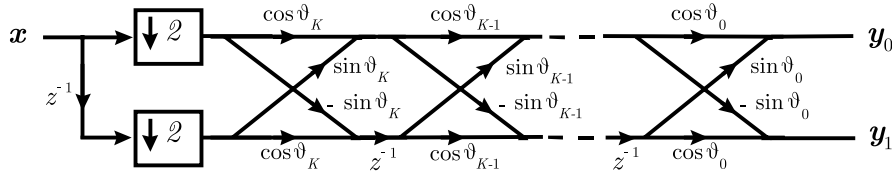


Figure 1.13: Lattice implementation of a two-channel NP analysis bank with input signal  $\mathbf{x}$  and output signals  $\mathbf{y}_0$  and  $\mathbf{y}_1$ .

Note that with  $H_1(z)|_{z=1} = 0$  (1.3.18) implies  $H_0(z)|_{z=-1} = 0$ . By (1.3.21) this yields  $H_0(z)|_{z=1} = \pm\sqrt{2}$  where we again assume a positive sign. Thus using (1.3.18) have that  $H_0(z)|_{z=1} = -H_1(z)|_{z=-1} = \sqrt{2}$ . Finally, these observations give along with the type one polyphase decompositions (1.3.11) and (1.3.12)

$$\mathbf{H}_{\text{pol}}(z)|_{z=1} = \frac{1}{\sqrt{2}} \begin{pmatrix} 1 & 1 \\ -1 & 1 \end{pmatrix}. \quad (1.5.40)$$

Since we have by (1.5.35) that

$$\mathbf{H}_{\text{pol}}(z)|_{z=1} = \begin{bmatrix} \cos(\sum_{i=0}^K \vartheta_i) & \sin(\sum_{i=0}^K \vartheta_i) \\ -\sin(\sum_{i=0}^K \vartheta_i) & \cos(\sum_{i=0}^K \vartheta_i) \end{bmatrix},$$

we obtain

$$\sum_{i=0}^K \vartheta_i \equiv \frac{\pi}{4} \pmod{2\pi}.$$

Let  $\vartheta_K$  be the residue of  $\frac{\pi}{4} - \sum_{i=0}^{K-1} \vartheta_i$  modulo  $2\pi$  in  $[0, 2\pi[$ . Then the space

$$\mathcal{P}^K = \{\boldsymbol{\vartheta} = (\vartheta_0, \dots, \vartheta_{K-1}) : \vartheta_i \in [0, \pi[ \}$$

can serve to parameterize all two-channel FIR NP filter banks of order  $N = 2K + 1$  with real filter coefficients and at least one vanishing moment of the highpass filter, i.e., a zero mean. To emphasize this parameterization, we will use the superscript  $\boldsymbol{\vartheta}$  later. For atoms of a binary tree, defined by a pair  $(j, k)$ , we use the notation  $\mathbf{q}_{j,k}(\boldsymbol{\vartheta})$  to show this dependence. For a parameterization with more than one vanishing moment of the highpass filter, we refer to the method of Zou et al. [82].

**Symmetry.** The parameter space contains also a symmetry which leads to redundancy in some settings. However, we cannot exploit this symmetry in our applications. Therefore, we only sketch some facts here and refer to [53] for a detailed discussion and proofs. It can be shown that half of the parameter space corresponds to wavelets which are time reversals of the other half. A subspace of the parameter space that covers all wavelets but exclude their time reversals is given by choosing  $\vartheta_{K-1}$  from the interval  $[0, \pi/2[$  and  $\vartheta_0, \dots, \vartheta_{K-2}$  from the interval  $[0, \pi[$ , see [53]. This may be useful in some settings as the parameter space is reduced, resulting in an easier optimization of the lattice angles, see Section ?? for an example.

**Implementation.** The lattice structure is accepted to offer the lowest implementation complexity among all known FIR NP structures with real filter coefficients, e.g., see [16, 70, 13, 14, 33, 47]. If  $\cos \vartheta_i \neq 0 \forall i$  in (1.5.35), then the rotation matrix can be expressed as

$$\mathbf{R}(\vartheta_i) = \cos \vartheta_i \begin{bmatrix} 1 & \alpha_i \\ -\alpha_i & 1 \end{bmatrix}, \quad \text{where } \alpha_i = \tan \vartheta_i.$$

The factors  $\cos \vartheta_i$  can be summarized to a common factor  $c$  of the lattice structure

$$c = \prod_{i=0}^K \cos \vartheta_i = \prod_{i=0}^K (1 + \alpha_i^2)^{-\frac{1}{2}}.$$

An implementation based on this observation is called the *two multiplier QMF lattice* [70]. The total number of multiplications is then given by  $2(K+1) + 1$  which is nearly halve as many as for the direct form when noting that the order of the corresponding filters is given by  $N = 2K + 1$ . Each lattice element operates at half of the input rate making the lattice structure very attractive for efficient implementations. When using the discretization by the *Coordinate Rotation Digital Computer-Algorithm* [78, 15] for the lattice angles in (1.5.35), another efficient implementation can be used which is described in [47].

Despite the increasing computational capabilities and decreasing size and cost of so-called *general-purpose computational components*, e.g., microprocessors and dedicated signal processing chips, special purpose designs are often needed in order to meet certain requirements. Such application specific requirements are often considered as *very large scale integration* (VLSI) metrics such as power consumption, computational area, and execution time. For the purpose of an efficient implementation of cascaded two-channel FIR NP filter banks in direct form [35], several architectures are known

which mainly differ in the way that intermediate results are stored and routed. For instance, implementations based on *systolic routing networks*, also called *Data Format Converters* [77], distributed memory [18], and implementations that use a minimum number of registers [45]. However, the effective algorithmic description of two-channel NP filter banks by the lattice structure allows for improved designs resulting in the most efficient VLSI architectures of these filter banks known [16, 13, 55, 14, 33]. Another advantage is that the NP property of (1.5.35) is structurally induced [73], that is, it remains NP even under lattice coefficient quantization [17] making it a perfect scheme for any fixed-point implementations.

**Design-Techniques.** Of course, since the lattice structure above remains NP regardless of the lattice angles, it is a suitable design tool for half band filters. Let  $H_0^\vartheta(e^{i\omega})$  be the lowpass analysis filter associated with the parameterized lattice structure and let  $\omega_s$  be the stopband edge (the lower bound of the stopband, i.e., the stopband lives on  $[\omega_s, \pi)$ ), then for an approximation of ideal filters, we have to find lattice angles which minimize  $\int_{\omega_s}^{\pi} |H_0^\vartheta(e^{i\omega})|^2 d\omega$ . That the passband behaves well is guaranteed due to the power symmetric property, see (1.3.21). The characteristics of the other filters can be obtained from this prototype by (1.3.18) and (1.3.23), respectively. For detailed descriptions of constraint design techniques in the Fourier domain based on the lattice structure we refer to [73, 70] since we are only interested in signal-adapted designs in the following. Note that the parameterization of the polyphase matrix (1.5.35) can also be implemented by *lifting steps*, also known as *ladder structure* in engineering [52], which are frequently used for designing non-paraunitary (*biorthogonal*) perfect reconstruction schemes, see [11] for details. However, in this thesis we will rely on the implementation based on the lattice structure due its availability in already existing very efficient architectures which are especially needed when dealing with algorithms for implantable low-power / low-voltage devices in the following. We also refer to literature for other constrained design procedures in the Fourier domain which are not appropriate for our purpose such as *spectral factorization* [70, 17, 76, 59].

Regularity is a smoothness property of continuous-time wavelets derived from infinitely iterated NP filters and the *Hölder exponent*<sup>2</sup> is a common measure for it, e.g., see [7].

---

<sup>2</sup>If  $f \in \mathcal{C}^n(\mathbb{R})$  but  $f \notin \mathcal{C}^{n+1}(\mathbb{R})$ , then its Hölder exponent  $s$  is given by

$$s = n + \inf_x \left( \liminf_{|d| \rightarrow 0} \frac{\log |f^{(n)}(x+d) - f^{(n)}(x)|}{\log |d|} \right).$$

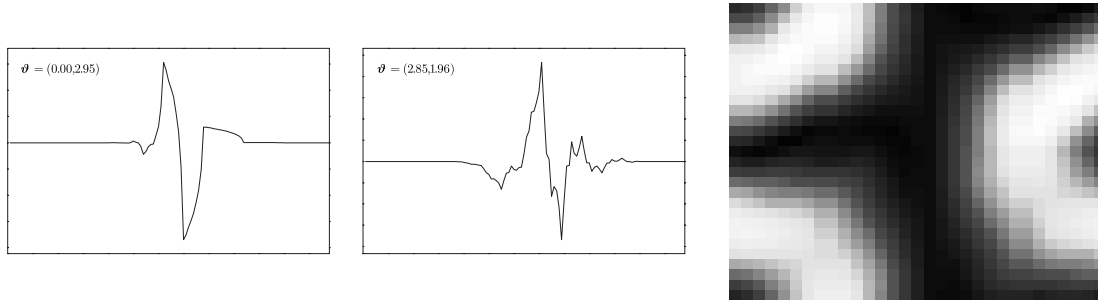


Figure 1.14: Left hand: two wavelets with distinct degree of second local variation. The smoother one, that is the atom with a lower second local variation, is the left one. Right hand: the matrix  $\mathbf{X}$ , the darker regions correspond to a lower variation, i.e., smoother wavelets.

The estimate of the smoothness of the continuous functions from the underlying filter has been addressed by several authors [10, 49, 7, 47, 36, 66]. But indeed, the only merit of regularity for practical tasks in digital signal processing is when smooth filters are need such as in image compression or hybrid pattern recognition and coding schemes where a reconstruction by non-smooth atoms may produce artifacts. However, here more straightforward measures can be used such as the  $\nu$ -local variation  $\chi_\nu$ , see [43, 38] and references therein, which is the  $\ell^1$  norm of the differences of  $\nu$ th order of a atom  $\mathbf{q}_{j,k}$  ( $j, k$  fixed). More precisely, let us denote the  $\nu$ th order differences by

$$D_\nu[\cdot; \mathbf{q}_{j,k}] = \sum_{i=0}^{\nu} (-1)^i \binom{\nu}{i} q_{j,k}[\cdot - i],$$

then we have that  $\chi_\nu(\mathbf{q}_{j,k}) = \|D_\nu[\cdot; \mathbf{q}_{j,k}]\|_{\ell^1}$ . Figure 1.14 (left hand) shows two atoms  $\mathbf{q}_{4,1}$  with distinct degrees of second local variation, i.e.,  $\nu = 2$ . The matrix  $\mathbf{X} = (\chi_2(\mathbf{q}_{4,1}(\vartheta_0, \vartheta_1)))_{\vartheta_0, \vartheta_1=0}^{\pi}$  which reflects the second order local variation of  $\mathbf{q}_{4,1}(\vartheta_0, \vartheta_1)$  in the parameter space is depicted in Figure 1.14 (right hand).

## 1.5.2 Lattice Optimization by Genetic Algorithms

In the subsequent chapters, we are interest in a lattice optimization for the purpose of pattern recognition. Throughout this thesis, we restrict ourselves to an optimization by some class separability criterion rather than direct classification performance that can be very time consuming for sophisticated learning machines which also involve large

optimization problems. Here a lattice optimization should provide an adaptation of time-scale atoms in the sense, that discriminatory information among signal classes is illuminated. Solving our subsequent lattice optimization problems analytically seems to be infeasible. The arising adaptation functionals seem not to allow for sophisticated calculus based strategies in the continuous parameter space. In particular, simple *hill climbing* methods are doomed to fail due to local minima of the adaptation functionals. Here we present two methods to cope with this problem.

**$\mu$ -Orthogonality.** Now we introduce a reduction strategy of the discretized parameter space. We introduce a discrete grid

$$\mathcal{P}_T^K = \{\boldsymbol{\vartheta} = (\vartheta_0, \dots, \vartheta_{K-1}) : \vartheta_i \in D\}, \quad D = \left\{ \frac{\pi\sigma}{T} : \sigma = 0, \dots, T-1 \right\}$$

in  $\mathcal{P}^K$ . Solving our adaptation tasks by evaluating the objective functions at each grid point is clearly one possibility which may be implemented for a small  $K$  and a coarse grid. However, for a larger  $K$  this can be time consuming. To cope with this problem, we have introduced a compression of the  $\mathcal{P}_T^K$  to obtain a sparse parameter space of atoms with a predefined degree of orthogonality to each other [62]. Given an arbitrary pair  $(j, k)$  of a binary tree and a positive number  $\mu < 1$ , we select a maximal subset  $\mathcal{P}_\mu^K$  of  $\mathcal{P}_T^K$  such that

$$|\langle \mathbf{q}_{j,k}(\boldsymbol{\vartheta}), \mathbf{q}_{j,k}(\overline{\boldsymbol{\vartheta}}) \rangle_{\ell^2}| \leq \mu, \quad \boldsymbol{\vartheta}, \overline{\boldsymbol{\vartheta}} \in \mathcal{P}_\mu^K \text{ with } \boldsymbol{\vartheta} \neq \overline{\boldsymbol{\vartheta}}. \quad (1.5.41)$$

The distinct atoms in (1.5.41) satisfy the *strengthened Cauchy-Schwarz inequality*, i.e., they are  $\mu$ -orthogonal. That is, the smaller  $\mu$  the more orthogonal are the atoms corresponding to  $\mathcal{P}_\mu^K$ . In a way,  $\mu$  steers the redundancy of our parameter space. Such a compression of the parameter space can be significant even for a large  $\mu$ . Indeed, for wavelets corresponding to an octave-band tree, we achieved a compression of  $|\mathcal{P}_\mu^K|/|\mathcal{P}_T^K| = 0.65$  if  $K = 2$ ,  $T = 32$  and  $\mu = 0.98$  on level  $j = 4$  in [62]. Such a large  $\mu$  does nearly not affect the adaptation flexibility since only atoms are discarded which result in relatively similar decompositions. However, the reduction of computation cost is tremendous as the example mentioned above shows.

**Genetic Algorithms.** The concept of *genetic algorithms* (GA) was firstly introduced by Holland [23]. Basically, genetic algorithms are stochastic search procedures often motivated by the mechanics of natural selection and genetics [23, 20]. Giving the gist "In nature, the individuals constituting a population adapt to the environment in which they live. The fittest individual have the highest probability of survival and tend to increase in numbers whereas less fit individual tend to die out. This survival of the fittest Darwinian principle is the idea of GA based search procedures".

Goldberg [20] pointed out the following four points in that GAs differ from conventional search or optimization procedures:

- GAs work with a coding set of parameters not with the parameters themselves.
- GAs search from a population of points, not from a single point.
- GAs use payoff (objective function) information, not derivatives or other auxiliary knowledge.
- GAs use probabilistic transition rules, not deterministic rules.

Accordingly, GAs are often described as a global search method that does not use gradient information and may be applied to nondifferentiable functions as well as functions with multiple local minima [80]. Here we only sketch some fundamentals of GAs and refer to [20, 40] for detailed discussions along with many examples of applications.

Assume we have to maximize an objective function given a search space. To apply GAs, the fundamental thing we have to do is to represent the search space by *artificial chromosomes* – known as the encoding of the problem. In the classical (*canonical*) GA, to which we restrict our interest here, these chromosomes are binary strings of length  $l$ . The first step for the GA is then to generate an initial population of size  $n$  of these chromosomes, i.e., an initial population of a number of  $n$  encoded candidate solutions to the problem. In the most common case, this initial population is generated randomly.

For our further discussions, it is helpful to consider the execution of a GA as a two stage process. It starts with a *current population* of size  $n$  (which is the initial population at the beginning). Then we wish to create the *next population* again of size  $n$  which hopefully will contain 'better' solutions to our problem. For this, we introduce an *intermediate population* between the current and the next population.

This intermediate population is created by applying a *selection operator* to the current population. Selection is a process in which individual chromosomes are copied according to their objective function values. In a way, now the "survival of the fittest strategy" comes into play. For this, the individual chromosomes of the current population are evaluated (by the objective function) and assigned with a so-called *fitness-value*. Here the fitness is defined by:  $f_i/\bar{f}$  where  $f_i$  is the evaluation associated with a particular chromosome  $i$  ( $i = 1, \dots, n$ ) and  $\bar{f}$  is the average evaluation associated with all  $n$  chromosomes of the population. Now the probability that chromosomes are copied and placed in the intermediate population is in proportion to their fitness. In other words, the probability that chromosomes with a higher fitness value are copied is also higher. Of course, in this selection the very same chromosome can be selected more than once.

To the intermediate population a *crossover operator* is applied. For this, all chromosomes in the population are mated at random. Then each pair of chromosomes undergoes a crossover with a predefined probability  $p_c$  in the following manner: an integer position  $k$  is selected uniformly at random between 1 and the chromosome length less one, i.e.,  $l - 1$ . Two new chromosomes are then created by swapping all the bits between positions  $k + 1$  and  $l$  inclusively. The resulting chromosomes form our next population. Now the next population becomes the current population and so on. It can be shown that the average fitness  $\bar{f}$  increases by a successive application these steps [20]. Each iteration of this process is called a *generation*.

Additionally to the crossover, there is optionally a *mutation operator* applied to intermediate population to create the next population. This operator flips some bits of a chromosome. Mutation can occur at each bit position in a chromosome with some probability  $p_m$ , usually very low, e.g., 0.01 or 0.001 [20, 40]. This operator introduces some noise in the main algorithm above and may help to escape from local minima.

As termination criteria for the GA described above, we may use the stabilization of GA (new generations do not improve the results) or a predefined number of iterations.

**Settings.** Throughout this thesis, we work with  $K = 2$  in (1.5.35). In this way, we obtain filters of order 5. The corresponding atoms have a relatively small support in time and may capture discriminating information in morphological structures of a short duration. Non-adapted filters of this order are frequently used in waveform recognition, e.g., see [4, 51]. Consequently, we have to optimize the lattice structure with respect to the angles  $\boldsymbol{\vartheta} = (\vartheta_0, \vartheta_1)$ . For all experiments, we use a  $l = 40$  bit

---

chromosome encoding for each angle in  $[0, \pi[$ . An initial population of  $n = 100$  is generated randomly. The probabilities for crossover and mutation are set to  $p_c = 0.95$  and  $p_m = 0.005$ , respectively. Such settings are common in practice [20, 40] and the GA stabilized with approximately 8 generations in average.

## 1.6 Conclusions

The theory of signal-adapted filter banks has been developed in recent years. Up to now, the underlying ideas mainly stick on this restricted area although they may have merit in other application fields such as machine learning.

In this chapter, we have presented the fundamentals needed for lattice structure based signal-adapted filter banks and time-scale atoms, respectively. We have in detail reviewed the theory of NP two-channel filter banks which can be used to realize decompositions of  $\ell^2$  into time-scale atoms. In particular, we have discussed octave-band multiresolution decomposition and wavelet packets.

We have shown that every NP two-channel FIR filter bank with real coefficients can be represented by the lattice structure. We have discussed the efficiency of the lattice structure for implementation and sketched some properties such as a zero mean constraint, a symmetry of the associated parameter space, and the design of smooth atoms.

In general, the optimization of the lattice angles represents a challenge in most settings [12, 59]. To cope with this problem, we have introduced two techniques, namely  $\mu$ -orthogonality and GAs. The former can be seen as a compression strategy for the lattice parameter space to obtain a more efficient sparse search space for atoms with a predefined degree of orthogonality to each other. In this way, all atoms which produce a similar decomposition are excluded from the parameter space. GAs are global search methods that only need objective function information. For applying them efficiently, the objective function must allow for a fast evaluation. For the optimization or adaptation of time-scale atoms, e.g., based on decomposition information, this fact is taken into account by the efficiency of the lattice structure.



# Bibliography

- [1] A. N. AAS AND C. T. MULLIS, *Minimum mean-square error transform coding and subband coding*, IEEE Trans. on Information Theory, 42 (1996), pp. 1179–1192.
- [2] N. AHMED AND R. K. RAO, *Orthogonal Transforms for Digital Signal Processing*, Springer-Verlag, NY, 1975.
- [3] A. AKANSU AND R. HADDAD, *Multiresolution Signal Decomposition*, Academic Press, NY, 1993.
- [4] M. AKAY, *Biomedical Signal Processing*, Academic Press, NY, 1994.
- [5] S. AKKARAKARAN AND P. P. VAIDYANATHAN, *Filter bank optimization with convex objectives, and the optimality of principal component forms*, IEEE Trans. on Signal Processing, 49 (2001), pp. 100–114.
- [6] M. BELLANGER, G. BONNEROT, AND M. COUDREUSE, *Digital filtering by polyphase network: application to sample rate alteration and filter banks*, IEEE Trans. on Acoust. Speech and Signal Proc., ASSP-24 (1976), pp. 109–114.
- [7] A. COHEN AND R. D. RYAN, *Wavelets and Multiscale Signal Processing*, Chapman & Hall, London, 1995.
- [8] R. R. COIFMAN AND M. V. WICKERHAUSER, *Entropy based algorithms for best basis selection*, IEEE Trans. on Information Theory, 32 (1992), pp. 712–718.
- [9] A. CROISIER, D. ESTEBAN, AND C. GALAND, *Perfect channel splitting by the use of interpolation/decimation/tree decomposition techniques*, Int. Conf. on Inform. Science and Systems, Patras, Greece, August 1976, pp. 443–446.

- [10] I. DAUBECHIES, *Ten Lectures on Wavelets*, SIAM, Philadelphia, PA, 1992.
- [11] I. DAUBECHIES AND W. SWELDENS, *Factoring wavelet transforms into lifting steps*, J. Fourier Anal. Appl., 4 (1998), pp. 245–267.
- [12] P. H. DELSARTE, B. MACQ, AND D. T. M. SLOCK, *Signal adapted multiresolution transforms for image coding*, IEEE Trans. on Information Theory, 38 (1992), pp. 897–903.
- [13] T. C. DENK AND K. K. PARHI, *Systematic design of architectures for M-ary tree structured filter banks*, in VLSI Signal Processing VIII, T. Nishitani and K. Parhi, eds., no. 1, Piscataway, NJ, October 1995, pp. 157–166.
- [14] ———, *Architectures for lattice structure based orthonormal discrete wavelet transform*, IEEE Trans. on Circuits and Systems II, 44 (1997), pp. 129–132.
- [15] E. F. DEPRETTERE AND A. DE LANGE, *The synthesis and implementation of signal processing application specific VLSI CORDIC arrays*, vol. 22 of Proceedings Int. Symp. Circuits and Systems, May 1990, pp. 974–977.
- [16] T. EDWARDS, *Discrete wavelet transform: Theory and implementation*, Technical Report, Information System Laboratory, Stanford University, 1992.
- [17] N. FLIEGE, *Multirate Digital Signal Processing*, John Wiley & Sons, NY, 1994.
- [18] J. FRIDMAN AND E. S. MANOLAKOS, *Distributed memory and control VLSI architectures for 1-D discrete wavelet transform*, in VLSI Signal Processing, no. 1, Piscataway, NJ, October 1995, pp. 157–166.
- [19] W. GIVENS, *Computation of plane unitary rotations transforming a general matrix to triangular form*, SIAM J. Appl. Math., 6 (1958), pp. 26–50.
- [20] D. E. GOLDBERG, *Genetic Algorithms in Search, Optimization, and Machine Learning*, Addison–Wesley, Reading, MA, 1989.
- [21] P. GOUPILLAUD, A. GROSSMANN, AND J. MORLET, *Cycle–octave and related transforms in seismic signal analysis*, Geoprospection, 23 (1984), pp. 85–102.
- [22] C. HERLEY, J. KOVAČEVIĆ, K. RAMCHANDRAN, AND V. M., *Tilings of the time–frequency plane: construction of arbitrary orthogonal bases and fast tiling algorithms*, IEEE Trans. on Signal Processing, 41 (1993), pp. 3341–3359.

- 
- [23] J. H. HOLLAND, *Adaptation in Natural and Artificial Systems*, University of Michigan Press, Ann Arbor MI, 1975.
- [24] A. HUANG AND P. M. SCHULTHEISS, *Block quantization of of correlated gaussian random variables*, IEEE Trans. on Comm. Systems, (September, 1963), pp. 289–296.
- [25] N. S. JAYANT AND P. NOLL, *Digital Coding of Waveforms*, Prentice Hall, Englewood Cliffs, NJ, 1984.
- [26] J. JUNG, D. J. STRAUSS, S. SIAPLAOURAS, A. BUOB, T. SINNWELL, Y. MANOLI, H. SCHIEFFER, AND A. HEISEL, *Wavelet analysis of bipolar endocardial electrograms for morphology based detection of ventricular tachycardias*, in IEEE Computers in Cardiology (26).
- [27] ———, *Detektion ventrikulärer tachykardien durch analyse des rechtsventrikulären bipolaren elektrogrammes*, in Jahrestagung der DGfK-HKF, Mannheim, Germany, 2000.
- [28] J. JUNG, D. J. STRAUSS, T. SINNWELL, G. HOHENBERG, R. FRIES, H. WERN, H. SCHIEFFER, AND A. HEISEL, *Identification of ventricular tachycardias by means of fast wavelet analysis*, in IEEE Computers in Cardiology (25), A. Murray and S. Swiryn, eds., NJ, 1998, pp. 21–24.
- [29] ———, *A new method for the discrimination of antegrade and retrograde atrial activation*, in Pacing and Clinical Electrophysiology, vol. 21, San Diego, CA, May 1998, p. 918.
- [30] ———, *Feasibility of wavelet transforms for discrimination of antegrade form retrograde atrial activation*, in Annals of Noninvasive Electrocardiology, vol. 3, 1998, p. 58.
- [31] ———, *Discrimination of antegrade and retrograde atrial activation by using wavelet transforms*, in A. des Maladies du Coeur et des Vaisseaux, vol. 91, 1998, p. 269.
- [32] ———, *Analysis of bipolar endocardial signals for discrimination of antegrade and retrograde atrial activation*, in European Heart J., vol. 12, 1998, p. 369.

- [33] J. T. KIM, Y. H. LEE, T. ISSHIKI, AND H. KUNIEDA, *Scalable VLSI architectures for lattice-structure-based discrete wavelet transform*, IEEE Trans. on Circuits and Systems II, 45 (1998), pp. 1031–1043.
- [34] A. KIRAC AND P. P. VAIDYANATHAN, *Theory and design of optimum FIR compaction filters*, IEEE Trans. on Signal Processing, 46 (1998), pp. 903–919.
- [35] G. KNOWLES, *VLSI architecture for the discrete wavelet transform*, Electron. Lett., EL-26 (1990), pp. 1184–1185.
- [36] A. K. LOUIS, P. MAASS, AND A. RIEDER, *Wavelets: Theory and Application*, John Wiley & Sons, Baffins Lane, Chichester, West Sussex, 1997.
- [37] S. MALLAT, *A theory for multiresolution signal decomposition*, IEEE Trans. on Pattern Recognition and Machine Intelligence, 11 (1989), pp. 674–693.
- [38] S. MASLAKOVIĆ, I. R. LINSOTT, M. OSICK, AND J. D. TWICKEN, *Smooth wavelet libraries: design and application*, Proc. IEEE Int. Conf. Acoust. Speech, and Signal Processing, Seattle, WA, May 1998, pp. 1793–1797.
- [39] F. MINTZER, *Filters for distortion-free two-band multirate filter banks*, IEEE Trans. on Acoust. Speech and Signal Proc., 33 (1985), pp. 626–630.
- [40] M. MITCHELL, *An introduction to Genetic Algorithms*, The MIT Press, Cambridge, MA, 1996.
- [41] P. MOULIN, M. ANITESCU, K. O. KORTANEK, AND F. A. POTRA, *The role of linear semi-infinite programming in signal-adapted qmf bank design*, IEEE Trans. on Signal Processing, 45 (1997), pp. 2160–2274.
- [42] P. MOULIN AND K. MIHÇAK, *Theory and design of signal-adapted FIR paraunitary filter banks*, IEEE Trans. on Signal Processing, 46 (1998), pp. 920–929.
- [43] J. E. ODEGARD AND C. S. BURRUS, *Discrete finite variation: A new measurement of wavelet smoothness for the design of wavelet basis*, Proc. IEEE Int. Conf. Acoust. Speech, and Signal Processing, Atlanta, GA, May 1996, pp. 1467–1470.
- [44] A. V. OPPENHEIM AND R. W. SCHAFER, *Discrete-Time Signal Processing*, Prentice Hall, Englewood Cliffs, NJ, 1989.

- 
- [45] K. K. PARTHI, *VLSI architecture for discrete wavelet transform*, IEEE Trans. on VLSI Systems., 1 (1993), pp. 191–202.
- [46] W. H. PRESS, S. A. TEUKOLSKY, W. T. VETTERLING, AND B. P. FLANNERY, *Numerical Recipes in C*, Cambridge University Press, Cambridge, 1992.
- [47] P. RIEDER, J. GÖTZE, J. A. NOSSEK, AND S. BURRUS, *Parameterization of orthogonal wavelet transform and their implementation*, IEEE Trans. on Circuits and Systems II, 45 (1998), pp. 217–226.
- [48] O. RIOUL, *A discrete-time multiresolution theory*, IEEE Trans. on Signal Processing, 41 (1993), pp. 2591–2606.
- [49] ———, *Regular wavelets: A discrete-time approach*, IEEE Trans. on Signal Processing, 41 (1993), pp. 3573–3579.
- [50] B. D. RIPLEY, *Pattern Recognition and Neural Networks*, Cambridge University Press, Cambridge, 1996.
- [51] N. SAITO AND R. R. COIFMAN, *Local discriminant bases and their applications*, J. Mathematical Imaging and Vision, 4 (1995), pp. 337–358.
- [52] I. SHAH AND T. A. C. M. KALKER, *On the ladder structure and linear phase conditions for bi-orthogonal filter banks*, in Proc. IEEE Int. Conf. Acoust. Speech, and Signal Processing, vol. 3, San Francisco, CA, October 1994, pp. 181–184.
- [53] B. G. SHERLOCK AND D. M. MONRO, *On the space of orthonormal wavelets*, IEEE Trans. on Signal Processing, 46 (1998), pp. 1716–1720. See also: C. Taswell. Correction for the Sherlock-Monro Algorithm for Generating the Space of Real Orthonormal Wavelets. Technical Report CT-1998-05, Computational Toolsmiths, 1998.
- [54] V. SILVA AND L. DE SÁ, *Analytical optimization of CQF filter banks*, IEEE Trans. on Signal Processing, 44 (1996), pp. 1564–1568.
- [55] S. SIMON, P. RIEDER, C. SCHIMPFLE, AND J. A. NOSSEK, *CORDIC-based architectures for the efficient implementation of discrete wavelet transform*, in Proc. ISCAS, vol. IV, Atlanta, GA, May 1996, pp. 77–80.

- [56] M. J. T. SMITH AND T. P. BARNWELL III, *A procedure for designing exact reconstruction filter banks for tree structured subband coders*, Proc. IEEE Int. Conf. Acoust. Speech, and Signal Processing, San Diego, CA, March 1984, pp. 27.1.1–27.1.4.
- [57] ———, *Exact reconstruction for tree-structured subband coders*, IEEE Trans. on Acoust. Speech and Signal Proc., 41 (1986), pp. 431–441.
- [58] A. K. SOMAN AND P. P. VAIDYANATHAN, *On orthonormal wavelets and paraunitary filter banks*, IEEE Trans. on Signal Processing, 41 (1993), pp. 1170–1183.
- [59] G. STRANG AND T. NGUYEN, *Wavelets and Filter Banks*, Wellesley–Cambridge Press, Wellesley, MA, 1996.
- [60] D. J. STRAUSS, J. JUNG, AND A. RIEDER, *The recognition of antegrade and retrograde atrial activation patterns using hybrid wavelet neural network schemes*, in IEEE Computers in Cardiology (26), A. Murray and S. Swiryn, eds., 2000, pp. 545–549.
- [61] D. J. STRAUSS, J. JUNG, A. RIEDER, AND Y. MANOLI, *Classification of endocardial electrograms using adapted wavelet packets and neural networks*, Annals of Biomedical Engineering, 29 (2001), pp. 483–492.
- [62] D. J. STRAUSS, T. SINNWELL, A. RIEDER, Y. MANOLI, AND J. JUNG, *A promising approach to morphological endocardial signal discriminations: Adapted multiresolution signal decompositions*, Applied Signal Processing, 6 (1999), pp. 182–193.
- [63] D. J. STRAUSS AND G. STEIDL, *Hybrid wavelet-support vector classifiers*, Preprint 264/01, 2001, Faculty of Mathematics and Computer Science, University of Mannheim, 2001.
- [64] D. J. STRAUSS, G. STEIDL, AND W. DELB, *Feature extraction by morphological local discriminant bases*, technical report tr-01-023, Faculty of Mathematics and Computer Science, University of Mannheim, 2001.
- [65] D. J. STRAUSS, G. STEIDL, AND J. JUNG, *Arrhythmia detection using signal-adapted wavelet preprocessing for support vector machines*, in IEEE Computers in Cardiology (28), A. Murray and S. Swiryn, eds., 2001, pp. 497–501.

- 
- [66] C. TASWELL, *Numerical evaluation of time-domain moments and regularity of multirate filter banks*, Proceedings of the 8th IEEE DSP workshop, August 1998. Paper # 71.
- [67] A. H. TEWFIK, D. SINHA, AND P. JORGENSEN, *On the optimal choice of a wavelet for signal representation*, IEEE Trans. on Information Theory, 38 (1992), pp. 747–765.
- [68] M. K. TSATSANIS AND G. B. GIANNAKIS, *Principal component filter banks for optimal multiresolution analysis*, IEEE Trans. on Signal Processing, 43 (1995), pp. 1766–1777.
- [69] P. P. VAIDYANATHAN, *Multirate digital filters, filter banks, polyphase networks, and applications: A tutorial*, in Proc. IEEE, vol. 78, January 1990, pp. 56–93.
- [70] ———, *Multirate Systems and Filter Banks*, Prentice Hall, Englewood Cliffs, NJ, 1993.
- [71] ———, *Theory of optimum orthonormal filter banks*, IEEE Trans. on Signal Processing, 46 (1998), pp. 1528–1543.
- [72] P. P. VAIDYANATHAN AND S. AKKARAKARAN, *A review of the theory and applications of principal component filter banks*, J. of Applied and Computational Harmonic Analysis. to appear.
- [73] P. P. VAIDYANATHAN AND P. Q. HOANG, *Lattice structures for optimal design and robust implementation of two-channel perfect reconstruction qmf filter banks*, IEEE Trans. Acoust. Speech, and Signal Proc., 36 (1988), pp. 81–94.
- [74] P. VARY, *On the design of digital filter banks based on a modified principle polyphase*, AEU, 33 (1979), pp. 293–300.
- [75] M. VETTERLI AND C. HERLEY, *Wavelets and filter banks: Theory and design*, IEEE Trans. on Signal Processing, 40 (1992), pp. 2207–2232.
- [76] M. VETTERLI AND J. KOVAČEVIĆ, *Wavelets and Subband Coding*, Prentice-Hall, Englewood Cliffs, NJ, 1995.

- [77] M. VISHWANATH, R. M. OWENS, AND M. J. IRWIN, *VLSI architecture for the discrete wavelet transform*, IEEE Trans. on Circuits and Systems II, 42 (1995), pp. 305–316.
- [78] J. E. VOLDER, *The CORDIC trigonometric computing technique*, IRE Trans. on Electronic Computers, 8 (1959), pp. 330–334.
- [79] S. WATANABE, *Knowing and Guessing*, Wiley, NY, 1969.
- [80] A. WHITLEY, *A genetic algorithm tutorial*, in Statistics and Computing, vol. 4, 1994, pp. 65–85.
- [81] M. V. WICKERHAUSER, *Adapted Wavelet Analysis from Theory to Software*, A. K. Peters, Ltd., Wellesley, MA, 1994.
- [82] H. ZOU AND A. H. TEWFIK, *Parameterization of compactly supported wavelets orthonormal wavelets*, IEEE Trans. on Signal Processing, 41 (1993), pp. 1428–1431.